ESAIM: M2AN 57 (2023) 1619–1655
https://doi.org/10.1051/m2an/2023029

ESAIM: Mathematical Modelling and Numerical Analysis
www.esaim-m2an.org

EFFICIENT INEQUALITY-PRESERVING INTEGRATORS FOR DIFFERENTIAL EQUATIONS SATISFYING FORWARD EULER CONDITIONS

Hong Zhang[1,*], Xu Qian[1], Jun Xia[2] and Songhe Song[1]

Abstract. Developing explicit, high-order accurate, and stable algorithms for nonlinear differential equations remains an exceedingly difficult task. In this work, a systematic approach is proposed to develop high-order, large time-stepping schemes that can preserve inequality structures shared by a class of differential equations satisfying forward Euler conditions. Strong-stability-preserving (SSP) methods are popular and effective for solving equations of this type. However, few methods can deal with the situation when the time-step size is larger than that allowed by SSP methods. By adopting time-step-dependent stabilization and taking advantage of integrating factor methods in the Shu–Osher form, we propose enforcing the inequality structure preservation by approximating the exponential function using a novel recurrent approximation without harming the convergence. We define sufficient conditions for the obtained parametric Runge–Kutta (pRK) schemes to preserve inequality structures for any time-step size, namely, the underlying Shu–Osher coefficients are non-negative. To remove the requirement of a large stabilization term caused by stiff linear operators, we further develop inequality-preserving parametric integrating factor Runge–Kutta (pIFRK) schemes by incorporating the pRK with an integrating factor related to the stiff term, and enforcing the non-decreasing of abscissas. The only free parameter can be determined a priori based on the SSP coefficient, the time-step size, and the forward Euler condition. We demonstrate that the parametric methods developed here offer an effective and unified approach to study problems that satisfy forward Euler conditions, and cover a wide range of well-known models. Finally, numerical experiments reflect the high-order accuracy, efficiency, and inequality-preserving properties of the proposed schemes.

Mathematics Subject Classification. 65L06, 65L20, 65M12, 35B50.

Received November 6, 2022. Accepted March 27, 2023.

1. Introduction

Consider an initial value problem for a system of $N \geq 1$ ordinary differential equations (ODEs) of the type

$$\begin{cases} u_t = f\big(t, u(t)\big), \quad \forall t \in (0, T], \\ u(0) = u^0, \end{cases} \tag{1.1}$$

Keywords and phrases. Inequality-preserving, Forward Euler condition, Strong-stability-preserving integrator, Fixed-point-preserving, Time-step-dependent stabilization.

[1] Department of Mathematics, National University of Defense Technology, Changsha 410073, P.R. China.
[2] College of Basic Education, National University of Defense Technology, Changsha 410073, P.R. China.
*Corresponding author: zhanghnudt@163.com

where $u^0 \in \mathbb{R}^N$, $f : \mathbb{R} \times \mathbb{R}^N \to \mathbb{R}^N$ is a continuous function. We assume that the problem (1.1) has a unique solution $u = [u_0, u_1, \ldots, u_{N-1}]^T : [0, T] \to \mathbb{R}^N$, and $\|\cdot\| : \mathbb{R}^N \to \mathbb{R}$ is a convex functional (*e.g.*, a norm or a semi-norm), such that

$$\|\alpha u + (1-\alpha)v\| \le \alpha\|u\| + (1-\alpha)\|v\|, \quad \forall \alpha \in [0,1], \quad \text{and} \quad u, v \in \mathbb{R}^N.$$

In the last three decades, many studies have been devoted to the development of high-order time integrators that can preserve the inequality structures of differential equations satisfying some forward Euler conditions [1]. Let $u^n \approx u(t_n)$ be the numerical solution at $t_n = n\tau$ computed by a method for (1.1) with time-step size τ, below we present the definitions of several properties of numerical integrators [1–4] for (1.1) that can be characterized by such conditions.

Definition 1.1 (Strong stability preservation/Monotonicity)**.** A method is strong-stability-preserving (monotone) with respect to the functional $\|\cdot\|$ if $\|u^n\| \le \|u^0\|$, $\forall n > 0$ under the assumption that

$$\exists \tau_{\mathrm{FE}} > 0, \text{ such that } \|u + \tau f(t,u)\| \le \|u\|, \quad \forall 0 < \tau \le \tau_{\mathrm{FE}}, \quad \forall t \in [0,T], \quad \forall \|u\| \le \|u^0\|. \tag{1.2}$$

Definition 1.2 (Positivity preservation)**.** A method is positive if whenever $u^0 \ge 0$, it guarantees that $u^n \ge 0$, $\forall n > 0$ under the assumption that

$$\exists \tau_{\mathrm{FE}} > 0, \text{ such that } u + \tau f(t,u) \ge 0, \quad \forall 0 < \tau \le \tau_{\mathrm{FE}}, \quad \forall t \in [0,T], \quad \forall u \ge 0, \tag{1.3}$$

where the inequalities are component-wise.

Definition 1.3 (Range boundedness/Maximum-principle preservation)**.** A method is range bounded (maximum-principle-preserving) in $[m, M]$ if whenever $m \le u^0 \le M$, it guarantees that $m \le u^n \le M$, $\forall n > 0$, under the assumption that

$$\exists \tau_{\mathrm{FE}} > 0, \text{ such that } m \le u + \tau f(t,u) \le M, \quad \forall 0 < \tau \le \tau_{\mathrm{FE}}, \quad \forall t \in [0,T], \quad \forall m \le u \le M, \tag{1.4}$$

where the inequalities are component-wise. When $M = -m := \beta > 0$, we define $\|u\|_{l^\infty} = \max_i |u_i|$, and then the assumption (1.4) becomes

$$\exists \tau_{\mathrm{FE}} > 0, \text{ such that } \|u + \tau f(t,u)\|_{l^\infty} \le \beta, \quad \forall 0 < \tau \le \tau_{\mathrm{FE}}, \quad \forall t \in [0,T], \quad \forall \|u\|_{l^\infty} \le \beta. \tag{1.5}$$

Definition 1.4 (Contractivity preservation)**.** A method is contractive if $\|u^n - v^n\| \le \|u^0 - v^0\|$, $\forall n > 0$, under the assumption that

$$\exists \tau_{\mathrm{FE}} > 0, \text{ such that } \|u - v + \tau\left(f(t,u) - f(t,v)\right)\| \le \|u - v\|, \quad \forall 0 < \tau \le \tau_{\mathrm{FE}}, \quad \forall t \in [0,T], \quad \forall u, v \in \mathbb{R}^N. \tag{1.6}$$

Typical problems which highly depend on above inequality-preserving integrators include the diminishing of total variation in fluid dynamics [5], the positivity of density and pressure [6], the range boundedness of solutions in hyperbolic equations [7, 8], and the maximum principle of order parameter in phase field models [4]. As the inequalities in Definitions 1.1–1.4 are characterized by forward Euler conditions (1.2)–(1.6), they can be preserved using the traditional SSP methods in most situations, as presented in the research of Hundsdorfer *et al.* [9], Ferracina and Spijker [10, 11], Higueras [12, 13], Gottlieb *et al.* [1]. Consider the preservation of strong stability in Definition 1.1. In the last three decades, significant efforts have been made to develop methods that reach the highest-order and admit the largest possible SSP coefficient $\mathcal{C}$ for prescribed stage or step numbers, such that a method can preserve strong stability under the condition $\tau \le \mathcal{C}\tau_{\mathrm{FE}}$. Nevertheless, there are restrictions on the attainable value of $\mathcal{C}$ for a given method, and SSP Runge–Kutta methods with non-negative coefficients have order barrier $p \le 4$ for explicit schemes, $p \le 6$ for implicit schemes [1, 2, 14]. Although, SSP multi-step schemes with non-negative coefficients have no order barrier [15, 16], they require many steps to reach a given high-order. For studies on conditionally SSP methods, see [1, 5, 14, 15, 17–19], and the references therein.

To remove restrictions on the time-step size, various studies have been focused on the development of unconditionally inequality-preserving schemes. Although the implicit Euler method can preserve strong stability without a time-step restriction (p. 10 in [9]), it has been proven that high-order implicit Runge–Kutta (RK) or linear multi-step (MS) methods cannot achieve this goal [9, 20]. Therefore, many ideas have been proposed beyond the traditional framework. The diagonally split Runge–Kutta methods (DSRK), which were originally introduced to unconditionally preserve the contractivity [21, 22], were adopted by Macdonald *et al.* [23] to preserve the strong stability. Unfortunately, it was shown that although second- and third-order unconditionally contractive DSRK methods preserved the strong stability for all time-step sizes, they suffered from order reduction at large step sizes. By incorporating negative coefficients and downwind-biased spatial discretization, Ketcheson [24] developed a class of second-order RK methods with an arbitrarily large SSP coefficient. Bonaventura and Della Rocca [3] proposed two unconditionally SSP extensions of the TR-BDF2 (trapezoidal rule-backward differentiation formula 2) method based on hybridization with the unconditionally SSP implicit Euler method, which can be activated using a sensor detecting violations of relevant functional bounds. Recently, by enforcing the backward derivative condition, Gottlieb *et al.* [25] proposed up to the fourth-order unconditionally SSP implicit two-derivative RK methods. Considering differential equations that have a special graph Laplacian structure, Blanes *et al.* [26] developed second-order methods that preserve positivity unconditionally and a third-order method that preserves positivity under very mild conditions. Other significant work in preserving the inequality structures was performed using the (modified) Patankar RK schemes [27–29].

To avoid solving implicit systems, explicit large time-stepping SSP schemes are desirable for numerically solving ODEs, and it is not surprising that such methods are difficult to construct. In this spirit, consider adding an $\mathcal{O}(\tau^2)$ term $\tau\kappa(u^n - u^{n+1})$ to the forward Euler formula $u^{n+1} = u^n + \tau f(t_n, u^n)$. Then we construct a first-order implicit–explicit (IMEX) Euler scheme

$$u^{n+1} = u^n + \tau[f(t_n, u^n) + \kappa u^n] - \tau\kappa u^{n+1}. \tag{1.7}$$

Assuming that $\kappa \geq \max\left\{\frac{1}{\tau_{\mathrm{FE}}} - \frac{1}{\tau}, 0\right\}$, then it holds that $\frac{\tau}{1+\tau\kappa} \leq \min\{\tau_{\mathrm{FE}}, \tau\} \leq \tau_{\mathrm{FE}}$. By using the forward Euler condition (1.2), we can derive the strong-stability preservation of (1.7):

$$\left\|u^{n+1}\right\| = \left\|u^n + \frac{\tau}{1+\tau\kappa} f(t_n, u^n)\right\| \leq \|u^n\|, \quad \forall \tau > 0.$$

We can see that if $\tau \leq \tau_{\mathrm{FE}}$, with the diminishing of κ, the IMEX Euler scheme (1.7) becomes the forward Euler scheme, thus retaining the accuracy of the original scheme. When $\tau > \tau_{\mathrm{FE}}$, the introduction of the stabilization term $\tau\kappa(u^n - u^{n+1})$ stabilizes the scheme and preserves the strong stability by rescaling the time-step size from τ to $\frac{\tau}{1+\tau\kappa} \leq \tau_{\mathrm{FE}}$. Although the construction of this first-order SSP method for any time-step size τ by adding an $\mathcal{O}(\tau^2)$ term with a time-step-dependent (TSD) parameter κ is direct, severe time delay exists because of the time step rescaling, and the extension of this idea to higher order schemes is not straightforward.

In addition to the maximum-principle preservation for (1.1) in Definition 1.3, the preservation of the maximum principle for stiff ODE systems in the form

$$\begin{cases} u_t = Lu + N(u), & t \in (0, T], \\ u(0) = u^0, \end{cases} \tag{1.8}$$

which are obtained by space discretization of Allen–Cahn-type (AC-type) equations, has attracted much attention in recent years. Du *et al.* [4] investigated sufficient conditions for the semilinear problem (1.8) to have a maximum principle by developing an abstract framework.

Assumption 1.1. [4, 30] *The matrix L is the generator of a contraction semigroup on $\mathbb{R}^N$; that is, $\|\mathrm{e}^{\tau L}\|_\infty \leq 1$, $\forall \tau > 0$, where $\|A\|_\infty = \sup_{\|u\|_{l^\infty}=1} \|Au\|_{l^\infty}$ denotes the induced infinity norm of a matrix $A \in \mathbb{R}^{N\times N}$.*

Assumption 1.2. [4] *The nonlinear operator N acts as a vector-valued function induced by a given continuously differentiable function $N_0 : \mathbb{R} \to \mathbb{R}$, that is $N(u) = [N_0(u_0), N_0(u_1), \ldots, N_0(u_{N-1})]^T \in \mathbb{R}^N$, and there exists a constant $\beta > 0$ such that*

$$N_0(\beta) \le 0 \le N_0(-\beta), \qquad \text{for some constant } \beta > 0.$$

Because of the change of sign on both sides of zero, a forward Euler condition on $N(u)$ [30] holds,

$$\exists \tilde{\tau}_{\mathrm{FE}} > 0, \text{ such that } \|u + \tau N(u)\|_{l^\infty} \le \beta, \quad \forall 0 < \tau \le \tilde{\tau}_{\mathrm{FE}}, \quad \forall \|u\|_{l^\infty} \le \beta. \tag{1.9}$$

Lemma 1.5. [4] *Assume L and $N(u)$ satisfy Assumptions 1.1 and 1.2, respectively. Then (1.8) admits the maximum principle: $\|u(t)\|_{l^\infty} \le \beta$, $\forall t > 0$ for any $\|u^0\|_{l^\infty} \le \beta$.*

Unlike studies on the inequality-preserving methods in Definitions 1.1–1.4, the maximum-principle preservation of (1.8) has been independently investigated from another perspective. By taking advantage of the forward Euler condition (1.5), Tang and Yang [31] proposed the first maximum-principle-preserving (MPP) scheme by using the IMEX Euler formula with the TSD stabilization technique. Later, by adopting the central finite difference for the diffusion term and upwind discretization for the advection term, Shen *et al.* [32] investigated an unconditionally MPP semi-implicit scheme with the TSD stabilization for the generalized AC equation. Recently, by using a fourth-order spatial finite-difference discretization, Shen and Zhang [33] proved that the stabilized IMEX scheme was MPP under a suitable mesh-size constraint. However, traditional high-order temporal integrators fail to unconditionally preserve the maximum principle because of a lack of strategies for dealing with the stiff term and the stabilization term.

When considering the preservation of strong stability of systems in the form (1.8), Isherwood *et al.* [34] noted that a forward Euler condition on the linear term Lu with respect to $\|\cdot\|$, that is,

$$\exists \bar{\tau}_{\mathrm{FE}} > 0, \text{ such that } \|u + \tau L u\| \le \|u\|, \quad \forall 0 < \tau \le \bar{\tau}_{\mathrm{FE}},$$

implies a contraction property $\|\mathrm{e}^{\tau L} u\| \le \|u\|$, $\forall \tau > 0$. Based on this finding, Isherwood *et al.* developed SSP integrating factor Runge–Kutta (IFRK) [34, 35] and integrating factor two-step Runge–Kutta (IFTSRK) [36] schemes that only require the time-step size to satisfy a forward Euler condition on the nonlinear term. The IFRK approach has also been investigated for the maximum-principle preservation of (1.8) in [30,37]. To remove the time step restriction in the preservation of the maximum principle, a circle condition has been frequently incorporated. Let $\kappa = \frac{1}{\tau} \ge \frac{1}{\tilde{\tau}_{\mathrm{FE}}}$, then the forward Euler condition (1.9) is equivalent to

$$\|\kappa u + N(u)\|_{l^\infty} \le \kappa\beta, \quad \forall \kappa \ge \frac{1}{\tilde{\tau}_{\mathrm{FE}}}, \quad \forall \|u\|_{l^\infty} \le \beta. \tag{1.10}$$

This so-called circle condition (1.10) [1,2,20] means that $N(u)$ is bounded by a 'circle' measured by $\|\cdot\|_{l^\infty}$ that is centered at $-\kappa u \in \mathbb{R}^N$ with radius $\kappa\beta$. By utilizing exponential time difference (ETD) methods and the circle condition, Du *et al.* [38] developed two unconditionally MPP schemes for the non-local AC equation, that is, the stabilized first-order ETD1 scheme and the second-order ETD2 scheme. The ETD schemes have become popular in recent years. Du *et al.* [4] further proved that stabilized ETD schemes can preserve the maximum-principle unconditionally for a class of semilinear parabolic equations, and Ju *et al.* [39] showed that the ETD2 scheme incorporated with the generalized SAV and stabilization techniques unconditionally dissipates the energy of AC-type gradient flows. The success of stabilized ETD schemes lies in the fact that the contraction semi-group property of L can be directly incorporated with the stabilization parameter κ in the temporal integrators, *i.e.*, $\|\mathrm{e}^{\tau(L-\kappa)} u\|_{l^\infty} \le \mathrm{e}^{-\tau\kappa} \|u\|_{l^\infty}$. This stabilization technique has been introduced to the IFRK framework, in which a class of up to third-order unconditionally MPP stabilized IFRK schemes was proposed by Li *et al.* [40]. Zhang *et al.* proposed to approximate exponential functions in the stabilized IFRK, IFTSRK (integrating factor two-step Runge–Kutta), and IFMS (integrating factor multi-step) schemes using different Taylor series [41, 42], recurrent approximations or combinations of exponential and linear functions [43, 44]. The resulting up to the

fourth-order parametric IFRK, eighth-order parametric IFTSRK, and arbitrarily high-order parametric IFMS schemes not only preserve the maximum-principle unconditionally but also conserve the mass for conservative AC-type equations.

Moreover, the stabilization technique was introduced to scalar hyperbolic equations with stiff source terms by Huang and Shu [8]. Starting from traditional pth-order stabilized integrating factor Runge–Kutta formulas in the Shu–Osher form, they proposed replacing exponential functions with pth- or $(p+1)$th-degree Taylor series to weaken the exponential effects produced by the stabilizing exponential term without destroying the convergence. Thus, the obtained high-order modified exponential SSP RK schemes only require the time-step size to satisfy the forward Euler condition on the nonlinear term, that is, $\tau \leq \mathcal{C}\tilde{\tau}_{\mathrm{FE}}$. In [45], Du *et al.* developed Taylor series approximation for stabilized integrating factor multi-step schemes. They constructed up to the third-order conservative, and bound-preserving schemes for stiff multispecies detonation. Later, Du *et al.* [46,47] proposed third-order modified exponential RK schemes in the Shu–Osher form by using conservative approximations comprising combinations of linear and exponential functions. To reduce the large truncation errors brought by the stabilization, Yang *et al.* [48] applied the standard RK scheme to the nonstiff equation and the modified exponential RK scheme to the stiff equation. If equations with different stiffness were encountered, they also considered applying the exponential RK method with a different stabilization parameter. This greatly improved the numerical accuracy. Still, the stabilization did not appear in the forward Euler condition of the nonlinear term, and the time-step size restriction existed.

In addition to the above studies on MPP and bound-preserving schemes using the stabilization technique, the idea of adding and subtracting a linear term has also been developed to improve the stability of numerical integrators, as demonstrated by Shen and Yang [49], as well as in earlier papers [50–55]. Examples include the introduction of $\kappa(u-u)$ to AC-type equations [49], $\kappa(\Delta u - \Delta u)$ to the mean-curvature or Cahn–Hilliard equations [51, 54, 56], $\kappa\left(\Delta^2 u - \Delta^2 u\right)$ to a surface diffusion equation [52] and a fourth-order image inpainting model [57], and $J_n(u-u)$ wtih $J_n = \frac{\partial f(t,u)}{\partial u}(u_n)$ to general nonlinear problem [58]. Such stabilization techniques were also referred to as Douglas splitting by Hundsdorfer [59], and the explicit–implicit-null (EIN) method by Duchemin and Eggers [60]. The first- and second-order EIN integrators were successfully incorporated with local discontinuous Galerkin discretizations to develop unconditionally stable schemes for nonlinear diffusion problems by Wang *et al.* [61]. To the best of our knowledge, there is still no stabilization method higher than first-order with a TSD stabilizer.

Since explicit, high-order accurate and stable schemes for both (1.1) and (1.8) are desirable, and a larger stabilization term introduces more truncation errors and time delay [48,62,63], the objective of this paper is to develop high-order inequality-preserving methods with TSD stabilization for both (1.1) and (1.8). The purpose is to increase the order (up to the fourth) and, simultaneously reduce additional truncation errors introduced by stabilization. To the best of our knowledge, there has been few study on explicit, high-order accurate and stable schemes to preserve inequality structures for (1.1), nor on direct incorporation of TSD stabilization in high-order schemes. Compared with the existing literature, the new contributions of this work include:

- Recurrent approximations for exponential functions are proposed to develop up to the fourth-order, large time-stepping and inequality-preserving parametric RK schemes with TSD stabilization.
- To tackle problems with both stiff and nonlinear terms, a family of explicit parametric integrating factor RK schemes that need small stabilization parameters are constructed to preserve the inequality structures.
- The inequality-preservation of the pRK schemes has relatively mild requirements on the stabilization parameter and underlying schemes, that is, the stabilizing parameter $\kappa \geq \max\{\frac{1}{\tau_{\mathrm{FE}}} - \frac{\mathcal{C}}{\tau}, 0\}$ and all coefficients are non-negative. The parametric integrating factor RK schemes further require that all abscissas are non-decreasing and $\kappa \geq \max\{\frac{1}{\tilde{\tau}_{\mathrm{FE}}} - \frac{\mathcal{C}}{\tau}, 0\}$.

The rest of this paper is organized as follows. In Section 2, we provide sufficient conditions for (1.1) to admit inequality structures in Definitions 1.1–1.4. In Section 3, we start with a fixed-point-preserving improvement over the traditional integrating factor method, and illustrate main idea to construct up to the fourth-order inequality-preserving single-step schemes with TSD stabilization. The linear stability analysis and convergence

estimate are carried out in Section 4. In Section 5, various experiments are performed to demonstrate the effectiveness and advantages of the proposed schemes. Some concluding remarks are presented in Section 6.

2. Preliminaries

Before constructing high-order schemes that can preserve the inequalities in Definitions 1.1–1.4 at time steps larger than that allowed by SSP integrator, we first provide sufficient conditions for (1.1) to have corresponding structures. By extending the analytical framework developed by Du *et al.* [4], the following result can be derived.

Lemma 2.1. *For the system (1.1), assume $f(t,u)$ is continuous with respect to both variables, satisfies one or more forward Euler conditions in (1.2)–(1.6), and meets corresponding Lipschitz conditions, that is, there exists a constant $K>0$, such that*

$$\text{Strong stability}: \quad \|f(t,u_1)-f(t,u_2)\|_* \le K\|u_1-u_2\|_*, \quad \forall t\in[0,T],\ \forall\|u_i\|\le\|u^0\|,\ i=1,2; \tag{2.1}$$

$$\text{Positivity}: \quad \|f(t,u_1)-f(t,u_2)\|_* \le K\|u_1-u_2\|_*, \quad \forall t\in[0,T],\ \forall u_i\ge 0,\ i=1,2; \tag{2.2}$$

$$\text{Range boundedness}: \quad \|f(t,u_1)-f(t,u_2)\|_* \le K\|u_1-u_2\|_*, \quad \forall t\in[0,T],\ \forall m\le u_i\le M,\ i=1,2; \tag{2.3}$$

$$\text{Maximum principle}: \quad \|f(t,u_1)-f(t,u_2)\|_* \le K\|u_1-u_2\|_*, \quad \forall t\in[0,T],\ \forall\|u_i\|_{l^\infty}\le\beta,\ i=1,2; \tag{2.4}$$

$$\text{Contractivity}: \quad \|f(t,u_1)-f(t,u_2)\|_* \le K\|u_1-u_2\|_*, \quad \forall t\in[0,T],\ \forall u_i\in\mathbb{R}^N, i=1,2. \tag{2.5}$$

Here, the symbol $\|\cdot\|_*$ can be any norm, e.g., the infinity-norm or the 2-norm. Then (1.1) has a unique solution $u\in C\left([0,T];\mathbb{R}^N\right)$ and admits the corresponding inequalities:

$$\text{Strong stability}: \quad \|u(t)\|\le\|u^0\|, \quad \forall t\in[0,T],\ \forall u^0\in\mathbb{R}^N; \tag{2.6}$$

$$\text{Positivity}: \quad u(t)\ge 0, \quad \forall t\in[0,T],\ \forall u^0\ge 0; \tag{2.7}$$

$$\text{Rangeboundedness}: \quad m\le u(t)\le M, \quad \forall t\in[0,T],\ \forall m\le u^0\le M; \tag{2.8}$$

$$\text{Maximumprinciple}: \quad \|u(t)\|_{l^\infty}\le\beta, \quad \forall t\in[0,T],\ \forall\|u^0\|_{l^\infty}\le\beta; \tag{2.9}$$

$$\text{Contractivity}: \quad \|u(t)-v(t)\|\le\|u^0-v^0\|, \quad \forall t\in[0,T],\ \forall u^0,v^0\in\mathbb{R}^N; \tag{2.10}$$

where the inequalities in (2.7) and (2.8) are component-wise, and $v(t)$ in (2.10) is the solution to (1.1) with initial condition v^0.

The proofs of (2.6)–(2.10) essentially follow that of Theorem 2.3 in [4]. For the completeness, we present it in Appendix A.

3. Inequality-preserving integrators with a time-step-dependent parameter

To construct efficient, accurate and stable time integration methods for general stiff, nonlinear differential equations, we follow previous studies [57, 64–67] and set out three key design principles. First, fixed points of the system are preserved. Second, the nonlinear term is handled simply and inexpensively. Third, the time-step size is selected to reflect the accuracy requirement, rather than restricted by the stability constraint. In this section, we develop a family of inequality-preserving parametric schemes that satisfy the above principles and are remarkably easy to implement.

3.1. Parametric Runge–Kutta schemes

Consider the stabilization technique studied in [4, 49, 51, 53, 60]. By introducing $\kappa(u-u),\ \kappa>0$ to the ODE system (1.1), we obtain an equivalent formulation

$$\begin{cases} u_t = f(t,u)+\kappa u-\kappa u, & \forall t\in(0,T], \\ u(0)=u^0. \end{cases} \tag{3.1}$$

TABLE 1. Order conditions for second- and third-order explicit RK schemes using Shu–Osher coefficients, and fourth-order schemes using Butcher coefficients.

RK(2, 2)	RK(3, 3)
$\sum_{j=0}^{i-1}\alpha_{i,j}=1,\ i=1,2$	$\sum_{j=0}^{i-1}\alpha_{i,j}=1,\ i=1,2,3$
$\alpha_{2,1}\beta_{1,0}+\sum_{j=0}^{1}\beta_{2,j}=1$	$\alpha_{3,1}\beta_{1,0}+\alpha_{3,2}c_2+\sum_{j=0}^{2}\beta_{3,i}=1$
$\beta_{2,1}\beta_{1,0}=\frac{1}{2}$	$\beta_{1,0}(\alpha_{3,2}\beta_{2,1}+\beta_{3,1})+\beta_{3,2}c_2=\frac{1}{2}$
	$\beta_{1,0}^2(\alpha_{3,2}\beta_{2,1}+\beta_{3,1})+\beta_{3,2}c_2^2=\frac{1}{3}$
	$\beta_{3,2}\beta_{2,1}\beta_{1,0}=\frac{1}{6}$
RK(s, 4)	
$b^T\mathbf{1}=1;\ b^Tc=\frac{1}{2};\ b^Tc^2=\frac{1}{3};\ b^TAc=\frac{1}{6};$	
$b^Tc^3=\frac{1}{4};\ b^T[c\cdot(Ac)]=\frac{1}{8};\ b^TAc^2=\frac{1}{12};\ b^TA^2c=\frac{1}{24}.$	

Here, $\mathbf{1}=[1,\dots,1]^T\in\mathbb{R}^s,\ c=[c_0,c_1,\dots,c_{s-1}]^T,\ A=[a_{i,j}]_{i,j=0,\dots,s-1}\in\mathbb{R}^{s\times s},\ b=[a_{s,0},a_{s,1},\dots,a_{s,s-1}]^T$, and powers of vectors are component-wise.

Assume the initial condition $u^0=u^*$ is a steady state to (3.1), *i.e.*, $f(t,u^*)=0$. It is expected that a numerical method will preserve the steady state.

An s-stage, pth-order explicit RK scheme for (3.1) can be presented in the Shu–Osher form [68],

$$\begin{cases} u_{n,0}=u^n, \\ u_{n,i}=\displaystyle\sum_{j=0}^{i-1}[\alpha_{i,j}u_{n,j}+\tau\beta_{i,j}f(t_{n,j},u_{n,j})] \\ \qquad\quad =\displaystyle\sum_{j=0}^{i-1}\alpha_{i,j}\left[u_{n,j}+\tau\frac{\beta_{i,j}}{\alpha_{i,j}}f(t_{n,j},u_{n,j})\right], \quad i=1,\dots,s, \\ u^{n+1}=u_{n,s}, \end{cases} \tag{3.2}$$

where $t_{n,j}=t_n+c_j\tau,\ \ c_i=\sum_{j=0}^{i-1}(\alpha_{i,j}c_j+\beta_{i,j}),\ \ \sum_{j=0}^{i-1}\alpha_{i,j}=1$, and non-negative coefficients $\alpha_{i,j},\beta_{i,j}$ are constrained by certain accuracy requirements [68,69]. The explicit Shu–Osher formulation can be written in the Butcher form

$$u_{n,i}=u^n+\tau\sum_{j=0}^{i-1}a_{i,j}f(t_{n,j},u_{n,j}), \quad i=1,\dots,s, \tag{3.3}$$

with Butcher coefficients given by [14],

$$a_{i,j}=\beta_{i,j}+\sum_{k=j+1}^{i-1}\alpha_{i,k}a_{k,j}, \quad i=1,\dots,s;\ j=0,\dots i-1. \tag{3.4}$$

For convenience, we present second- and third-order conditions [1] using Shu–Osher coefficients, and fourth-order conditions [70] using Butcher coefficients in Table 1.

For an SSP RK scheme, we assume a given $\alpha_{i,j}$ is zero only if its corresponding $\beta_{i,j}$ is zero. If we denote the SSP coefficient by $\mathcal{C}=\min_{i,j}\frac{\alpha_{i,j}}{\beta_{i,j}}>0$ (the ratio is understood as infinite if $\beta_{i,j}=0$), since the formulation (3.2) is a convex combination of the forward Euler steps $u_{n,j}+\tau\frac{\beta_{i,j}}{\alpha_{i,j}}f(t_{n,j},u_{n,j})$, the inequalities in Definitions 1.1–1.4 are preserved by traditional SSP RK schemes for any $\tau\in(0,\mathcal{C}\tau_{\mathrm{FE}}]$.

To remove the restriction on the time-step size, let us apply the Lawson transformation [71] to the unknown $u(t)$, *i.e.*, $v(t) = \mathrm{e}^{\kappa t}u(t)$. Then we obtain an equivalent system of the stabilized formulation (3.1)

$$\begin{cases} v_t = \mathrm{e}^{\kappa t}\left[f\left(t, \mathrm{e}^{-\kappa t}v\right) + \kappa \mathrm{e}^{-\kappa t}v\right], \quad t \in (0, T], \\ v(0) = u^0. \end{cases} \tag{3.5}$$

Applying the Shu–Osher formulation (3.2) to problem (3.5) and using the inverse transformation $u(t) = \mathrm{e}^{-\kappa t}v(t)$ yield the Shu–Osher IFRK method:

$$u_{n,i} = \sum_{j=0}^{i-1} \mathrm{e}^{-(c_i - c_j)\tau\kappa}\left(\alpha_{i,j}u_{n,j} + \tau\beta_{i,j}\left[f(t_{n,j}, u_{n,j}) + \kappa u_{n,j}\right]\right), \quad i = 1, \ldots, s. \tag{3.6}$$

Assuming $u_{n,j} = u^*, j = 0, \ldots, i-1$, we obtain

$$\begin{aligned} u_{n,i} &= \frac{1}{\mathrm{e}^{c_i\tau\kappa}} \sum_{j=0}^{i-1} \mathrm{e}^{c_j\tau\kappa}\left(\alpha_{i,j}u^* + \tau\beta_{i,j}\left[\underbrace{f(t_{n,j}, u^*)}_{=0} + \kappa u^*\right]\right) \\ &= \frac{1}{\mathrm{e}^{c_i\tau\kappa}} \sum_{j=0}^{i-1} \mathrm{e}^{c_j\tau\kappa}\left(\alpha_{i,j} + \tau\kappa\beta_{i,j}\right)u^*, \quad i \le s. \end{aligned}$$

Note that the denominator $\mathrm{e}^{c_i\tau\kappa}$ will not equal the numerator $\sum_{j=0}^{i-1}\mathrm{e}^{c_j\tau\kappa}(\alpha_{i,j} + \tau\kappa\beta_{i,j})$ unless $c_i\tau\kappa = 0$. Therefore, IFRK (3.6) cannot preserve fixed points unless u^* is a zero vector. To solve this problem, let $\psi_0(\tau\kappa) := 1$, we propose approximating the exponential functions $\mathrm{e}^{c_i\tau\kappa}$ using

$$\psi_i(\tau\kappa) := \sum_{j=0}^{i-1} \psi_j(\tau\kappa)(\alpha_{i,j} + \tau\kappa\beta_{i,j}), \quad i = 1, \ldots, s. \tag{3.7}$$

Then we get the modification in the Shu–Osher form

$$u_{n,i} = \frac{1}{\psi_i(\tau\kappa)} \sum_{j=0}^{i-1} \psi_j(\tau\kappa)\left(\alpha_{i,j}u_{n,j} + \tau\beta_{i,j}\left[f(t_{n,j}, u_{n,j}) + \kappa u_{n,j}\right]\right) \tag{3.8}$$

$$= \sum_{j=0}^{i-1}\left(\hat{\alpha}_{i,j}(\tau\kappa)u_{n,j} + \tau\hat{\beta}_{i,j}(\tau\kappa)f(t_{n,j}, u_{n,j})\right), \quad i = 1, \ldots, s, \tag{3.9}$$

where

$$\hat{\alpha}_{i,j}(\tau\kappa) = \frac{\psi_j(\tau\kappa)}{\psi_i(\tau\kappa)}(\alpha_{i,j} + \tau\kappa\beta_{i,j}), \qquad \hat{\beta}_{i,j}(\tau\kappa) = \frac{\psi_j(\tau\kappa)}{\psi_i(\tau\kappa)}\beta_{i,j}. \tag{3.10}$$

We denote (3.9) [equivalent to (3.8)] as the parametric RK method (pRK), and the parametric abscissas are calculated using $\hat{c}_i(\tau\kappa) = \sum_{j=0}^{i-1}\left[\hat{\alpha}_{i,j}(\tau\kappa)\hat{c}_j(\tau\kappa) + \hat{\beta}_{i,j}(\tau\kappa)\right]$, $i = 1, \ldots, s$. Clearly, pRK preserves fixed points and are explicit.

Remember that the Shu–Osher coefficients can be transformed to the Butcher coefficients using the relationship (3.4), we have the following result.

Lemma 3.1. *Assume the Butcher coefficients $a_{i,j}$ in (3.11) are transformed from underlying Shu–Osher coefficients $\alpha_{i,j}, \beta_{i,j}$ in (3.8), then the approximations $\psi_i(\tau\kappa)$ (3.7) can be reformulated using the Butcher coefficients as*

$$\psi_i(\tau\kappa) = 1 + \tau\kappa\sum_{j=0}^{i-1} a_{i,j}\psi_j(\tau\kappa), \quad i = 1, \ldots, s.$$

Proof. We prove this by induction. Let I^s be the identity matrix in $\mathbb{R}^{s\times s}$. Note that $a_{k,j} = 0, j \geq k$, and $\psi_0(\tau\kappa) = 1$, we assume $\psi_k(\tau\kappa) = 1 + \tau\kappa \sum_{j=0}^{k-1} a_{k,j}\psi_j(\tau\kappa),\ k = 1, \ldots, i-1$. By using the transformation (3.4), we derive

$$\begin{aligned}
\psi_i(\tau\kappa) &= \sum_{j=0}^{i-1} \psi_j(\tau\kappa)\left[\alpha_{i,j} + \tau\kappa\beta_{i,j}\right] \\
&= \sum_{j=0}^{i-1} \psi_j(\tau\kappa)\left[\alpha_{i,j} + \tau\kappa\left(a_{i,j} - \sum_{k=0}^{i-1}\alpha_{i,k}a_{k,j}\right)\right] \\
&= \sum_{j=0}^{i-1} \psi_j(\tau\kappa)\left[\alpha_{i,j} - \tau\kappa\sum_{k=0}^{i-1}\alpha_{i,k}a_{k,j}\right] + \tau\kappa\sum_{j=0}^{i-1} a_{i,j}\psi_j(\tau\kappa) \\
&= \sum_{k=0}^{i-1} \alpha_{i,k}\left[\sum_{j=0}^{i-1}(I^s_{k,j} - \tau\kappa a_{k,j})\psi_j(\tau\kappa)\right] + \tau\kappa\sum_{j=0}^{i-1} a_{i,j}\psi_j(\tau\kappa) \\
&= \sum_{k=0}^{i-1}\left(\alpha_{i,k}\left[\psi_k(\tau\kappa) - \tau\kappa\sum_{j=0}^{k-1} a_{k,j}\psi_j(\tau\kappa)\right]\right) + \tau\kappa\sum_{j=0}^{i-1} a_{i,j}\psi_j(\tau\kappa) \\
&= \sum_{k=0}^{i-1}\alpha_{i,k} + \tau\kappa\sum_{j=0}^{i-1} a_{i,j}\psi_j(\tau\kappa) \\
&= 1 + \tau\kappa\sum_{j=0}^{i-1} a_{i,j}\psi_j(\tau\kappa), \quad i \leq s.
\end{aligned}$$

This completes the proof. □

By using the equivalence between the Shu–Osher IFRK formulation (3.6) and the following Butcher IFRK formulation

$$u_{n,i} = \mathrm{e}^{-c_i\tau\kappa}\left(u^n + \tau\sum_{j=0}^{i-1} a_{i,j}\mathrm{e}^{c_j\tau\kappa}\left[f(t_{n,j}, u_{n,j}) + \kappa u_{n,j}\right]\right), \quad i = 1, \ldots, s,$$

we rewrite the parametric RK scheme in the Butcher form

$$u_{n,i} = \frac{1}{\psi_i(\tau\kappa)}\left(u^n + \tau\sum_{j=0}^{i-1} a_{i,j}\psi_j(\tau\kappa)\left[f(t_{n,j}, u_{n,j}) + \kappa u_{n,j}\right]\right) \tag{3.11}$$

$$= u^n + \tau\sum_{j=0}^{i-1}\hat{a}_{i,j}(\tau\kappa)f(t_{n,j}, u_{n,j}) \quad i = 1, \ldots, s, \tag{3.12}$$

where $\hat{a}_{i,j}(\tau\kappa)$ are explicitly transformed by

$$\hat{a}_{i,j}(\tau\kappa) = \frac{1}{\psi_i(\tau\kappa)}\left[a_{i,j}\psi_j(\tau\kappa) + \tau\kappa\sum_{k=j+1}^{i-1} a_{i,k}\psi_k(\tau\kappa)\hat{a}_{k,j}(\tau\kappa)\right], \quad i = 1, \ldots, s;\ j = 0, \ldots, i-1.$$

TABLE 2. Order conditions for explicit pRK schemes (m ranges from 0 to the degree of $\tilde{c}_m$).

Order conditions using parametric Butcher coefficients					
Tree	Term	Order 1	Order 2	Order 3	Order 4
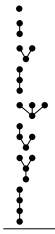	τ	$\hat{b}^T\mathbf{1}-1=\mathcal{O}(\tau\kappa)$	$\hat{b}^T\mathbf{1}-1=\mathcal{O}(\tau^2\kappa^2)$	$\hat{b}^T\mathbf{1}-1=\mathcal{O}(\tau^3\kappa^3)$	$\hat{b}^T\mathbf{1}-1=\mathcal{O}(\tau^4\kappa^4)$
	τ^2		$\hat{b}^T\tilde{c}_m-\frac{1}{2}=\mathcal{O}(\tau\kappa)$	$\hat{b}^T\tilde{c}_m-\frac{1}{2}=\mathcal{O}(\tau^2\kappa^2)$	$\hat{b}^T\tilde{c}_m-\frac{1}{2}=\mathcal{O}(\tau^3\kappa^3)$
	τ^3			$\hat{b}^T\tilde{c}_m^2-\frac{1}{3}=\mathcal{O}(\tau\kappa)$	$\hat{b}^T\tilde{c}_m^2-\frac{1}{3}=\mathcal{O}(\tau^2\kappa^2)$
	τ^3			$\hat{b}^T\hat{A}\tilde{c}_m-\frac{1}{6}=\mathcal{O}(\tau\kappa)$	$\hat{b}^T\hat{A}\tilde{c}_m-\frac{1}{6}=\mathcal{O}(\tau^2\kappa^2)$
	τ^4				$\hat{b}^T\tilde{c}_m^3-\frac{1}{4}=\mathcal{O}(\tau\kappa)$
	τ^4				$\hat{b}^T[\tilde{c}_{m_1}\cdot(\hat{A}\tilde{c}_{m_2})]-\frac{1}{8}=\mathcal{O}(\tau\kappa)$
	τ^4				$\hat{b}^T\hat{A}\tilde{c}_m^2-\frac{1}{12}=\mathcal{O}(\tau\kappa)$
	τ^4				$\hat{b}^T\hat{A}^2\tilde{c}_m-\frac{1}{24}=\mathcal{O}(\tau\kappa)$

Order conditions using parametric Shu–Osher coefficients		
Term	pRK(2, 2)	pRK(3, 3)
	$\sum_{j=0}^{i-1}\hat{\alpha}_{i,j}-1=0,\ i=1,2$	$\sum_{j=0}^{i-1}\hat{\alpha}_{i,j}-1=0,\ i=1,2,3$
τ	$\hat{\alpha}_{2,1}\hat{\beta}_{1,0}+\sum_{j=0}^{1}\hat{\beta}_{2,j}-1=\mathcal{O}(\tau^2\kappa^2)$	$\hat{\alpha}_{3,1}\hat{\beta}_{1,0}+\hat{\alpha}_{3,2}\hat{c}_2+\sum_{j=0}^{2}\hat{\beta}_{3,j}-1=\mathcal{O}(\tau^3\kappa^3)$
τ^2	$\hat{\beta}_{2,1}\hat{\beta}_{1,0}^{i}\beta_{1,0}^{1-i}-\frac{1}{2}=\mathcal{O}(\tau\kappa),\ i=0,1$	$\hat{\beta}_{1,0}^{i}\beta_{1,0}^{1-i}(\hat{\alpha}_{3,2}\hat{\beta}_{2,1}+\hat{\beta}_{3,1})+\hat{\beta}_{3,2}\hat{c}_2^{i}c_2^{1-i}-\frac{1}{2}=\mathcal{O}(\tau^2\kappa^2),\ i=0,1$
τ^3		$\hat{\beta}_{1,0}^{i}\beta_{1,0}^{2-i}(\hat{\alpha}_{3,2}\hat{\beta}_{2,1}+\hat{\beta}_{3,1})+\hat{\beta}_{3,2}\hat{c}_2^{i}c_2^{2-i}-\frac{1}{3}=\mathcal{O}(\tau\kappa),\ i=0,1,2$
τ^3		$\hat{\beta}_{3,2}\hat{\beta}_{2,1}\hat{\beta}_{1,0}^{i}\beta_{1,0}^{1-i}-\frac{1}{6}=\mathcal{O}(\tau\kappa),\ i=0,1$

The parametric Butcher tableau of pRK is given by

$$\begin{array}{cc|c} c & \hat{c} & \hat{A} \\ \hline c_s & \hat{c}_s & \hat{b}^T \end{array} = \begin{array}{cc|cccc} c_0 & \hat{c}_0 & 0 & 0 & 0 & 0 \\ c_1 & \hat{c}_1 & \hat{a}_{1,0} & 0 & 0 & 0 \\ \vdots & \vdots & \vdots & \vdots & \ddots & \\ c_{s-1} & \hat{c}_{s-1} & \hat{a}_{s-1,0} & \hat{a}_{s-1,1} & \cdots & 0 \\ \hline c_s & \hat{c}_s & \hat{a}_{s,0} & \hat{a}_{s,1} & \cdots & \hat{a}_{s,s-1} \end{array}, \tag{3.13}$$

where $\hat{c}_i(\tau\kappa)=\sum_{j=0}^{i-1}\hat{a}_{i,j}(\tau\kappa)$. We then study the accuracy of pRK schemes. To prove the pth order convergence of pRK, it is sufficient to prove consistency of order p (see, *e.g.*, Theorem 2.3.4 of [72]).

Lemma 3.2. *Assume the system (1.1) has an exact solution $u\in C^{p+1}\left([0,T];\mathbb{R}^N\right)$ and $u^n=u(t_n)$. If the pRK meets the pth-order conditions in Table 2, then the pRK (3.9) as applied to (1.1) has a $(p+1)$th order truncation error, that is,*

$$u^{n+1}-u(t_{n+1})=\mathcal{O}\left(\tau^{p+1}\sum_{k=0}^{p}\kappa^k\right)=\mathcal{O}(\tau^{p+1}).$$

Proof. To derive order conditions for the pRK scheme, we consider its Butcher form (3.12) on an ODE $u_t=f(t,u)$, and apply the Taylor expansions to obtain

$$u(t_{n,i})=u(t_n)+\sum_{k=1}^{p}\frac{(c_i\tau)^k}{k!}u^{(k)}(t_n)+\mathcal{O}\left(\tau^{p+1}\right),\quad i=1,\dots,s, \tag{3.14}$$

$$f\left(t_{n,j},u(t_{n,j})\right)=\sum_{k=1}^{p}\frac{(c_j\tau)^{k-1}}{(k-1)!}u^{(k)}(t_n)+\mathcal{O}(\tau^p),\quad j=1,\dots,s, \tag{3.15}$$

where $u^{(k)}(t_n):=\frac{\mathrm{d}^k u}{\mathrm{d}t^k}|_{t_n}$.

Inserting the exact solutions in the numerical scheme (3.12) gives

$$u(t_{n,i})=u(t_n)+\tau\sum_{j=0}^{i-1}\hat{a}_{i,j}f\left(t_{n,j},u(t_{n,j})\right)+\Delta_{n,i},\quad i=1,\dots,s. \tag{3.16}$$

Substituting (3.14) and (3.15) into (3.16) gives the defects

$$\Delta_{n,i} = \sum_{k=1}^{p} \tau^k \left(\frac{c_i^k}{k!} - \frac{1}{(k-1)!} \sum_{j=0}^{i-1} \hat{a}_{i,j} c_j^{k-1} \right) u^{(k)}\left(t_n\right) + \mathcal{O}(\tau^{p+1}), \quad i = 1, \ldots, s. \tag{3.17}$$

Denoting $e_{n,i} = u_{n,i} - u(t_{n,i}),\ i = 0, \ldots, s$, then $e^n = e_{n,0},\ e^{n+1} = e_{n,s}$. Subtracting (3.16) from (3.12) gives

$$e_{n,i} = e^n + \tau \sum_{j=0}^{i-1} \hat{a}_{i,j} \delta_{n,j} - \Delta_{n,i}, \quad i = 1, \ldots, s, \tag{3.18}$$

where $\delta_{n,j} = f(t_{n,j}, u_{n,j}) - f\left(t_{n,j}, u(t_{n,j})\right)$ are the right-hand-side stage errors. We assume an expansion for $\delta_{n,j}$ as a power series in τ,

$$\delta_{n,j} = \sum_{k=0}^{p-1} \delta_{n,j,k} \tau^k + \mathcal{O}(\tau^p). \tag{3.19}$$

Denoting the "error factors" of the defects $\Delta_{n,i}$ (3.17) as $\tau_{i,k} = \frac{c_i^k}{k!} - \frac{1}{(k-1)!} \sum_{j=0}^{i-1} \hat{a}_{i,j} c_j^{k-1}$, substituting the expansions (3.17) and (3.19) into the formula (3.18) yields

$$e_{n,i} = e^n + \sum_{k=0}^{p-1} \sum_{j=0}^{i-1} \hat{a}_{i,j} \delta_{n,j,k} \tau^{k+1} - \sum_{k=1}^{p} \tau^k \tau_{i,k} u^{(k)}(t_n) + \mathcal{O}(\tau^{p+1}), \quad i = 1, \ldots, s.$$

Hence the pRK method is consistent of order p if

$$\sum_{j=0}^{i-1} \hat{a}_{s,j} \delta_{n,j,k} = \mathcal{O}\left(\tau^{p-k} \kappa^{p-k}\right), \quad k = 0, \ldots, p-1;$$

$$\tau_{s,k} = \frac{c_s^k}{k!} - \frac{1}{(k-1)!} \hat{b}^T c^{k-1} = \mathcal{O}\left(\tau^{p+1-k} \kappa^{p+1-k}\right), \quad k = 1, \ldots, p.$$

We then relate $\delta_{n,j}$ recursively to $e_{n,j}$. Note that

$$\begin{aligned} \delta_{n,j} = f\left(t_{n,j}, u_{n,j}\right) - f\left(t_{n,j}, u(t_{n,j})\right) &= \sum_{m=1}^{\infty} \frac{1}{m!} \left(u_{n,j} - u(t_{n,j})\right)^m f^{(m)}\left(t_{n,j}, u(t_{n,j})\right) \\ &= \sum_{m=1}^{\infty} \frac{1}{m!} (e_{n,j})^m \bar{f}_m(t_{n,j}), \end{aligned}$$

where

$$\bar{f}_m(t_{n,j}) := f^{(m)}\left(t_{n,j}, u(t_{n,j})\right) = \frac{\partial^m}{\partial u^m} f|_{t_{n,j}, u(t_{n,j})}.$$

Since

$$\bar{f}_m(t_{n,j}) = \sum_{l=0}^{\infty} \frac{\tau^l}{l!} c_j^l \bar{f}_m^{(l)}(t_n).$$

We obtain the expansion of $\delta_{n,j}$ as

$$\delta_{n,j} = \sum_{m=1}^{\infty} \sum_{l=0}^{\infty} \frac{\tau^l}{m!l!} c_j^l (e_{n,j})^m \bar{f}_m^{(l)}(t_n).$$

Hence, the order conditions contain both c_j and $\hat{c}_j$. Let us define

$$\tilde{c}^k_{j,m} = c_j^m \hat{c}_j^{k-m}, \quad \tilde{c}^k_m = \left[\tilde{c}^k_{0,m}, \ldots, \tilde{c}^k_{s-1,m}\right]^T, \quad m = 0, \ldots, k.$$

By using the rooted trees theory [70], we present the second- to fourth-order conditions in Table 2. Noting that the Butcher modification can be transformed to the Shu–Osher modification, we also give the order conditions of pRK(2, 2) and pRK(3, 3) in Table 2 using the parametric Shu–Osher coefficients.

In the error expansion, each of these residuals is multiplied by the $\mathcal{O}(\tau^k)$ term in the "Term" column of Table 2, then the overall truncation error is $\mathcal{O}(\tau^{p+1}\sum_{k=0}^{p}\kappa^k)$, which is $\mathcal{O}(\tau^{p+1})$ after absorbing κ. For an N-dimensional system of ODEs, the truncation error is derived using the same approach by transition to multidimensional linear operators. □

Next, we consider the pRK(2, 2), pRK(3, 3) and pRK(4, 4) schemes to show that the pRK schemes retain the original convergence orders of underlying RK schemes. By applying conditions $\sum_{j=0}^{i-1}\alpha_{i,j} = 1,\ i = 1, \ldots, s,\ c_i = \sum_{j=0}^{i-1}(\alpha_{i,j}c_j + \beta_{i,j}),\ i = 1, \ldots, s$, and the transformation (3.4), we compute the approximations to exponential functions $\mathrm{e}^{c_i\tau\kappa},\ i = 1, 2, 3$ using Shu–Osher coefficients and $\mathrm{e}^{c_4\tau\kappa}$ using Butcher coefficients as below.

$$\begin{aligned}
\psi_1(\tau\kappa) &= \alpha_{1,0} + \tau\kappa\beta_{1,0} = 1 + \tau\kappa\beta_{1,0},\\
\psi_2(\tau\kappa) &= \alpha_{2,0} + \alpha_{2,1}\psi_1 + \tau\kappa\left(\beta_{2,0} + \beta_{2,1}\psi_1\right)\\
&= \alpha_{2,0} + \alpha_{2,1} + \tau\kappa\left[\alpha_{2,1}\beta_{1,0} + \beta_{2,0} + \beta_{2,1}\alpha_{1,0}\right] + (\tau\kappa)^2\beta_{2,1}\beta_{1,0},\\
&= 1 + \tau\kappa c_2 + (\tau\kappa)^2\beta_{2,1}\beta_{1,0},\\
\psi_3(\tau\kappa) &= \alpha_{3,0} + \alpha_{3,1}\psi_1 + \alpha_{3,2}\psi_2 + \tau\kappa\left[\beta_{3,0} + \beta_{3,1}\psi_1 + \beta_{3,2}\psi_2\right]\\
&= \left[\alpha_{3,0} + \alpha_{3,1} + \alpha_{3,2}\right]\\
&\quad + \tau\kappa\left[\alpha_{3,1}\beta_{1,0} + \alpha_{3,2}\left(\alpha_{2,1}\beta_{1,0} + \beta_{2,0} + \beta_{2,1}\alpha_{1,0}\right) + \beta_{3,0} + \beta_{3,1}\alpha_{1,0} + \beta_{3,2}\left(\alpha_{2,0} + \alpha_{2,1}\right)\right]\\
&\quad + (\tau\kappa)^2\left[\alpha_{3,2}\beta_{2,1}\beta_{1,0} + \beta_{3,1}\beta_{1,0} + \beta_{3,2}\left(\alpha_{2,1}\beta_{1,0} + \beta_{2,0} + \beta_{2,1}\alpha_{1,0}\right)\right] + (\tau\kappa)^3\beta_{3,2}\beta_{2,1}\beta_{1,0}\\
&= 1 + \tau\kappa\left(\alpha_{3,1}\beta_{1,0} + \alpha_{3,2}c_2 + \sum_{j=0}^{2}\beta_{3,i}\right) + (\tau\kappa)^2\left[\beta_{1,0}\left(\alpha_{3,2}\beta_{2,1} + \beta_{3,1}\right) + \beta_{3,2}c_2\right] + (\tau\kappa)^3\beta_{3,2}\beta_{2,1}\beta_{1,0}\\
&= 1 + \tau\kappa c_3 + (\tau\kappa)^2\left[\beta_{1,0}\left(\alpha_{3,2}\beta_{2,1} + \beta_{3,1}\right) + \beta_{3,2}c_2\right] + (\tau\kappa)^3\beta_{3,2}\beta_{2,1}\beta_{1,0},\\
\psi_4(\tau\kappa) &= 1 + c_4\tau\kappa + b^Tc(\tau\kappa)^2 + b^TAc(\tau\kappa)^3 + b^TA^2c(\tau\kappa)^4.
\end{aligned}$$

For fixed value of κ, verification of second-order conditions for pRK(2, 2) is done as follows:

$$\begin{aligned}
\sum_{j=0}^{i-1}\hat{\alpha}_{i,j} &= \sum_{j=0}^{i-1}\frac{\psi_j}{\psi_i}(\alpha_{i,j} + \tau\kappa\beta_{i,j}) = 1, \qquad i = 1, 2,\\
\hat{\alpha}_{2,1}\hat{\beta}_{1,0} + \sum_{j=0}^{1}\hat{\beta}_{2,j} &= \frac{\psi_1}{\psi_2}\left(\alpha_{2,1} + \tau\kappa\beta_{2,1}\right)\frac{1}{\psi_1}\beta_{1,0} + \frac{1}{\psi_2}\beta_{2,0} + \frac{\psi_1}{\psi_2}\beta_{2,1}\\
&= \frac{1}{\psi_2}\left[\alpha_{2,1}\beta_{1,0} + \beta_{2,0} + \beta_{2,1} + \tau\kappa\left(\beta_{2,1}\beta_{1,0} + \beta_{2,1}\beta_{1,0}\right)\right]\\
&= \frac{1 + \tau\kappa}{1 + \tau\kappa + \frac{1}{2}(\tau\kappa)^2} = 1 + \mathcal{O}\left(\tau^2\kappa^2\right),\\
\hat{\beta}_{1,0} &= \frac{\psi_1}{\psi_2}\frac{1}{\psi_1}\beta_{2,1}\beta_{1,0} = \frac{1}{2(1 + \tau\kappa + \frac{1}{2}(\tau\kappa)^2)} = \frac{1}{2} + \mathcal{O}(\tau\kappa).
\end{aligned}$$

Other conditions containing $\beta_{1,0}$ in Table 2 can be verified similarly.

Verification of third-order conditions for pRK(3, 3) is done as follows:

$$\sum_{j=0}^{i-1} \hat{\alpha}_{i,j} = 1, \quad i = 1,\, 2,\, 3.$$

$$\begin{aligned}
\sum_{j=0}^{i-1} \hat{\beta}_{3,j} + \hat{\alpha}_{3,1}\hat{\beta}_{1,0} + \hat{\alpha}_{3,2}\hat{c}_2 &= \frac{1}{\psi_3}\beta_{3,0} + \frac{\psi_1}{\psi_3}\beta_{3,1} + \frac{\psi_2}{\psi_3}\beta_{3,2} + \frac{\psi_1}{\psi_3}\left(\alpha_{3,1} + \tau\kappa\beta_{3,1}\right)\frac{\beta_{1,0}}{\psi_1} \\
&\quad + \frac{\psi_2}{\psi_3}(\alpha_{3,2} + \tau\kappa\beta_{3,2})\left[\frac{\psi_1}{\psi_2}\left(\alpha_{2,1} + \tau\kappa\beta_{2,1}\right)\frac{1}{\psi_1}\beta_{1,0} + \frac{1}{\psi_2}\beta_{2,0} + \frac{\psi_1}{\psi_2}\beta_{2,1}\hat{\alpha}_{1,0}\right] \\
&= \frac{1}{\psi_3}\left(\beta_{3,0} + \psi_1\beta_{3,1} + \psi_2\beta_{3,2}\right) + \frac{1}{\psi_3}\left(\alpha_{3,1}\beta_{1,0} + \tau\kappa\beta_{3,1}\beta_{1,0}\right) \\
&\quad + \frac{1}{\psi_3}\left(\alpha_{3,2} + \tau\kappa\beta_{3,2}\right)\left[\left(\alpha_{2,1} + \tau\kappa\beta_{2,1}\right)\beta_{1,0} + \beta_{2,0} + \psi_1\beta_{2,1}\hat{\alpha}_{1,0}\right] \\
&= \frac{1}{\psi_3}\left(\beta_{3,0} + \beta_{3,1}\alpha_{1,0} + \beta_{3,2}\left(\alpha_{2,0} + \alpha_{2,1}\right) + \alpha_{3,1}\beta_{1,0} + \alpha_{3,2}c_2\right. \\
&\quad + \tau\kappa\left[\beta_{3,1}\beta_{1,0} + \beta_{3,2}c_2 + \beta_{3,1}\beta_{1,0} + \beta_{3,2}c_2 + \alpha_{3,2}\left(\beta_{2,1}\beta_{1,0} + \beta_{2,1}\beta_{1,0}\right)\right] \\
&\quad \left.+(\tau\kappa)^2\left(3\beta_{3,2}\beta_{2,1}\beta_{1,0}\right)\right) \\
&= \frac{1}{1 + \tau\kappa + \frac{1}{2}(\tau\kappa)^2 + \frac{1}{6}(\tau\kappa)^3}\left[1 + \tau\kappa + \frac{1}{2}(\tau\kappa)^2\right] = 1 + \mathcal{O}(\tau^3\kappa^3),
\end{aligned}$$

$$\begin{aligned}
\hat{\beta}_{1,0}\left(\hat{\alpha}_{3,2}\hat{\beta}_{2,1} + \hat{\beta}_{3,1}\right) + \hat{\beta}_{3,2}\hat{c}_2 &= \frac{\beta_{1,0}}{\psi_1}\left[\frac{\psi_2}{\psi_3}\left(\alpha_{3,2} + \tau\kappa\beta_{3,2}\right)\frac{\psi_1}{\psi_2}\beta_{2,1} + \frac{\psi_1}{\psi_3}\beta_{3,1}\right] \\
&\quad + \frac{\psi_2}{\psi_3}\beta_{3,2}\left[\frac{\psi_1}{\psi_2}\left(\alpha_{2,1} + \tau\kappa\beta_{2,1}\right)\frac{1}{\psi_1}\beta_{1,0} + \frac{1}{\psi_2}\beta_{2,0} + \frac{\psi_1}{\psi_2}\beta_{2,1}\hat{\alpha}_{1,0}\right] \\
&= \frac{1}{\psi_3}\left[\alpha_{3,2}\beta_{2,1}\beta_{1,0} + \beta_{3,1}\beta_{1,0} + \beta_{3,2}c_2 + 3\tau\kappa\beta_{3,2}\beta_{2,1}\beta_{1,0}\right] \\
&= \frac{1}{1 + \tau\kappa + \frac{1}{2}(\tau\kappa)^2 + \frac{1}{6}(\tau\kappa)^3}\left[\frac{1}{2} + \frac{1}{2}\tau\kappa\right] \\
&= \frac{1}{2} + \mathcal{O}(\tau^2\kappa^2),
\end{aligned}$$

$$\begin{aligned}
\hat{\beta}_{1,0}^2(\hat{\alpha}_{3,2}\hat{\beta}_{2,1} + \hat{\beta}_{3,1}) + \hat{\beta}_{3,2}\hat{c}_2{}^2 &= \left(\frac{\beta_{1,0}}{\psi_1}\right)^2\left[\frac{\psi_2}{\psi_3}\left(\alpha_{3,2} + \tau\kappa\beta_{3,2}\right)\frac{\psi_1}{\psi_2}\beta_{2,1} + \frac{\psi_1}{\psi_3}\beta_{3,1}\right] \\
&\quad + \frac{\psi_2}{\psi_3}\beta_{3,2}\left[\frac{\psi_1}{\psi_2}(\alpha_{2,1} + \tau\kappa\beta_{2,1})\frac{1}{\psi_1}\beta_{1,0} + \frac{1}{\psi_2}\beta_{2,0} + \frac{\psi_1}{\psi_2}\beta_{2,1}\hat{\alpha}_{1,0}\right]^2 \\
&= \left(\beta_{1,0} + \mathcal{O}(\tau\kappa)\right)^2\left[\alpha_{3,2}\beta_{2,1} + \beta_{3,1} + \mathcal{O}(\tau\kappa)\right] + \left(\beta_{3,2} + \mathcal{O}(\tau\kappa)\right)\left[c_2 + \mathcal{O}(\tau\kappa)\right]^2 \\
&= \beta_{1,0}^2\left(\alpha_{3,2}\beta_{2,1} + \beta_{3,1}\right) + \beta_{3,2}c_2^2 + \mathcal{O}(\tau\kappa) = \frac{1}{3} + \mathcal{O}(\tau\kappa),
\end{aligned}$$

$$\hat{\beta}_{3,2}\hat{\beta}_{2,1}\hat{\beta}_{1,0} = \frac{\psi_2}{\psi_3}\frac{\psi_1}{\psi_2}\frac{1}{\psi_1}\beta_{3,2}\beta_{2,1}\beta_{1,0} = \frac{1}{6} + \mathcal{O}(\tau\kappa).$$

Other conditions containing $\beta_{1,0}$ and c_2 in Table 2 can be verified similarly.

Verification of the fourth-order conditions with $m = 0$ for pRK(4, 4) is carried out using the Butcher coefficients and done as follows:

$$
\begin{aligned}
\hat{b}^T\mathbf{1} = \hat{c}_4 &= \frac{c_4 + 2b^Tc\tau\kappa + 3b^TAc(\tau\kappa)^2 + 4b^TA^2c(\tau\kappa)^3}{1 + c_4\tau\kappa + b^Tc(\tau\kappa)^2 + b^TAc(\tau\kappa)^3 + b^TA^2c(\tau\kappa)^4} \\
&= \frac{1 + \tau\kappa + \frac{1}{2}(\tau\kappa)^2 + \frac{1}{6}(\tau\kappa)^3}{1 + \tau\kappa + \frac{1}{2}(\tau\kappa)^2 + \frac{1}{6}(\tau\kappa)^3 + \frac{1}{24}(\tau\kappa)^4} = 1 + \mathcal{O}(\tau^4\kappa^4), \\
\hat{b}^T\hat{c} &= \frac{b^Tc + 3b^TAc\tau\kappa + 6b^TA^2c(\tau\kappa)^2}{1 + c_4\tau\kappa + b^Tc(\tau\kappa)^2 + b^TAc(\tau\kappa)^3 + b^TA^2c(\tau\kappa)^4} \\
&= \frac{\frac{1}{2} + \frac{1}{2}\tau\kappa + \frac{1}{4}(\tau\kappa)^2}{1 + \tau\kappa + \frac{1}{2}(\tau\kappa)^2 + \frac{1}{6}(\tau\kappa)^3 + \frac{1}{24}(\tau\kappa)^4} = \frac{1}{2} + \mathcal{O}(\tau^3\kappa^3), \\
\hat{b}^T\hat{A}\hat{c} &= \frac{b^TAc + 4b^TA^2c\tau\kappa}{1 + c_4\tau\kappa + b^Tc(\tau\kappa)^2 + b^TAc(\tau\kappa)^3 + b^TA^2c(\tau\kappa)^4} \\
&= \frac{\frac{1}{6} + \frac{1}{6}\tau\kappa}{1 + \tau\kappa + \frac{1}{2}(\tau\kappa)^2 + \frac{1}{6}(\tau\kappa)^3 + \frac{1}{24}(\tau\kappa)^4} = \frac{1}{6} + \mathcal{O}(\tau^2\kappa^2), \\
\hat{b}^T\hat{c}^3 &= b^Tc^3 + \mathcal{O}(\tau\kappa), \quad \hat{b}^T[\hat{c}\cdot(\hat{A}\hat{c})] = b^T[c\cdot(Ac)] + \mathcal{O}(\tau\kappa), \quad \hat{b}^T\hat{A}\hat{c}^2 = b^TAc^2 + \mathcal{O}(\tau\kappa), \quad \hat{b}^T\hat{A}^2\hat{c} = b^TA^2c + \mathcal{O}(\tau\kappa).
\end{aligned}
$$

For the conditions $\hat{b}^T\tilde{c}_m^2 = \frac{1}{3} + \mathcal{O}(\tau^2\kappa^2)$, $m = 0, 1, 2$ of pRK(4, 4) and all other conditions, we verify them for each Butcher tableau appearing in this work in repository [73]. It shows that the pRK scheme retains the original convergence order of underlying RK scheme, but the truncation error depends on κ and τ. Thus the smaller is κ, the better is the accuracy. We point out that this is a common phenomenon of exponential integrators [74], although the exponential functions in IFRK are replaced by polynomial functions in pRK.

Theorem 3.3. *For the system (3.1), assume $f(t,u)$ meets one or more condition in (1.2)–(1.6), the underlying Shu–Osher coefficients are non-negative, and the SSP coefficient $\mathcal{C} \geq 0$. Then, for any time step $\tau > 0$, the pRK method (3.8) preserves the corresponding inequalities in Definitions 1.1–1.4, provided that*

$$
\kappa \geq \max\left\{\frac{1}{\tau_{\mathrm{FE}}} - \frac{\mathcal{C}}{\tau}, 0\right\}. \tag{3.20}
$$

Proof. Consider the preservation of strong stability as an example. We prove this by induction. When κ satisfies (3.20) and $\alpha_{i,j}^2 + \beta_{i,j}^2 \neq 0$, we have

$$
\frac{\tau\beta_{i,j}}{\alpha_{i,j} + \tau\kappa\beta_{i,j}} = \frac{1}{\frac{\alpha_{i,j}}{\tau\beta_{i,j}} + \kappa} \leq \frac{1}{\frac{\mathcal{C}}{\tau} + \kappa} \leq \tau_{\mathrm{FE}}. \tag{3.21}
$$

The pRK formulation (3.8) is equivalent to

$$
u_{n,i} = \frac{1}{\psi_i(\tau\kappa)}\sum_{j=0}^{i-1}\psi_j(\tau\kappa)(\alpha_{i,j} + \tau\kappa\beta_{i,j})\left[u_{n,j} + \frac{\tau\beta_{i,j}}{\alpha_{i,j} + \tau\kappa\beta_{i,j}}f(t_{n,j}, u_{n,j})\right], \quad i = 1, \ldots, s.
$$

Assume $\|u_{n,j}\| \leq \|u^n\|$, $j = 0, \ldots, i-1$; by using (3.21) and applying the forward Euler condition (1.2) and definitions of $\psi_i(\tau\kappa)$, we obtain

$$
\begin{aligned}
\|u_{n,i}\| &\leq \frac{1}{\psi_i(\tau\kappa)}\sum_{j=0}^{i-1}\psi_j(\tau\kappa)(\alpha_{i,j} + \tau\kappa\beta_{i,j})\left\|u_{n,j} + \frac{\tau\beta_{i,j}}{\alpha_{i,j} + \tau\kappa\beta_{i,j}}f(t_{n,j}, u_{n,j})\right\| \\
&\leq \frac{1}{\psi_i(\tau\kappa)}\sum_{j=0}^{i-1}\psi_j(\tau\kappa)(\alpha_{i,j} + \tau\kappa\beta_{i,j})\|u_{n,j}\| \\
&\leq \|u^n\|, \quad i \leq s.
\end{aligned}
$$

Thus $\|u^{n+1}\| = \|u_{n,s}\| \leq \|u^n\|$. Other properties in Definitions 1.1–1.4 can be proved similarly. □

Note that there is no explicit four-stage, fourth-order SSP RK scheme with $\mathcal{C} > 0$ [2,14,75], and no explicit RK scheme higher than the fourth order has positive SSP coefficient [2,75]. The unique four-stage, fourth-order accurate explicit RK scheme with non-negative Butcher coefficients is the classical RK(4, 4) scheme with $\mathcal{C} = 0$ (p. 521 in [2]). Therefore, the explicit pRK approach can give at most fourth-order accurate inequality-preserving integrators for any positive time step.

We present some non-negative RK formulas up to the fourth order with SSP coefficients below.

$$\text{RK}(1,1): \begin{array}{c|c} 0 & 0 \\ \hline 1 & 1 \end{array}, \qquad \text{RK}(2,2): \begin{array}{c|cc} 0 & 0 & 0 \\ 1 & 1 & 0 \\ \hline 1 & \frac{1}{2} & \frac{1}{2} \end{array}, \tag{3.22}$$

Forward Euler scheme, $\mathcal{C} = 1$ Heun's second-order scheme [68], $\mathcal{C} = 1$

$$\begin{array}{c|ccc} 0 & 0 & 0 & 0 \\ 1 & 1 & 0 & 0 \\ \frac{1}{2} & \frac{1}{4} & \frac{1}{4} & 0 \\ \hline 1 & \frac{1}{6} & \frac{1}{6} & \frac{2}{3} \end{array}, \qquad \begin{array}{c|cccc} 0 & 0 & 0 & 0 & 0 \\ \frac{1}{2} & \frac{1}{2} & 0 & 0 & 0 \\ \frac{1}{2} & 0 & \frac{1}{2} & 0 & 0 \\ 1 & 0 & 0 & 1 & 0 \\ \hline 1 & \frac{1}{6} & \frac{1}{3} & \frac{1}{3} & \frac{1}{6} \end{array},$$

RK(3,3) [68], $\mathcal{C} = 1$ RK(4, 4), $\mathcal{C} = 0$

RK(5, 4) [17], $\mathcal{C} \approx 1.50818004918983$, $c \approx [0, 0.3918, 0.5861, 0.4745, 0.9350]^T$:

$$\begin{cases} u_{n,1} = u_{n,0} + 0.391752226571890\tau f(t_{n,0}, u_{n,0}), \\ u_{n,2} = 0.444370493651235u_{n,0} + 0.555629506348765u_{n,1} + 0.368410593050371\tau f(t_{n,1}, u_{n,1}), \\ u_{n,3} = 0.620101851488403u_{n,0} + 0.379898148511597u_{n,2} + 0.251891774271694\tau f(t_{n,2}, u_{n,2}), \\ u_{n,4} = 0.178079954393132u_{n,0} + 0.821920045606868u_{n,3} + 0.544974750228521\tau f(t_{n,3}, u_{n,3}), \\ u^{n+1} = 0.517231671970585u_{n,2} + 0.096059710526147u_{n,3} + 0.063692468666290\tau f(t_{n,3}, u_{n,3}) \\ \qquad + 0.386708617503268u_{n,4} + 0.226007483236906\tau f(t_{n,4}, u_{n,4}). \end{cases} \tag{3.23}$$

Remark 3.4. Different from the classic RK Butcher tableaux, the pRK(s, p) Butcher tableau (3.13) depends on both the original abscissas c_i and the parametric abscissas $\hat{c}_i$. Since we interpret the solution $u_{n,s}$ of (3.12) as an approximation to $u(t_n + \tau)$ and the proposed approximation guarantees that $\hat{c}_s = \frac{c_s + \sum_{k=1}^{s-1}(k+1)b^T A^{k-1} c(\tau\kappa)^k}{1 + c_s\tau\kappa + \sum_{k=2}^{s} b^T A^{k-2} c(\tau\kappa)^k} = 1 + \mathcal{O}(\tau^p \kappa^p)$, $\forall \kappa \geq 0$, the time inconsistency is inevitable unless $\kappa = 0$. Thus the essence of the stabilization method is to trade consistency for stability (inequality-preservation) when $\tau > \mathcal{C}\tau_{\text{FE}}$, which is an effective and mainstream strategy in the construction of high-order stable schemes for stiff and nonlinear problems [4,8,46,49]. Nevertheless, the pRK can reach the fourth-order convergence in preserving inequality structures and the TSD stabilization $\kappa = \max\left\{\frac{1}{\tau_{\text{FE}}} - \frac{\mathcal{C}}{\tau}, 0\right\}$ makes good use of the original SSP coefficient $\mathcal{C}$ and has no influence on the accuracy when $\tau \leq \mathcal{C}\tau_{\text{FE}}$, hence pRK successfully reduces the time inconsistency comparing with existing stabilization schemes that use a constant parameter $\kappa \geq \frac{1}{\tau_{\text{FE}}}$ (presented in Sec. 3.3). In the literature, Ju *et al.* [39] pointed out that larger time step size leads to less accurate solutions in stabilization ETD-SAV schemes, and Li *et al.* [76] noted that stabilization would slow down the convergence rate. Although pRK is inequality-preserving for any time step, the time step size should be restricted by the desired accuracy instead of being arbitrarily large. Therefore, we call the proposed pRK schemes as efficient inequality-preserving rather than unconditionally inequality-preserving.

3.2. Parametric methods for systems with both stiff and nonlinear components

Now let us re-consider the system with both stiff and nonlinear terms in the form

$$u_t = Lu + N(t, u), \quad \forall t \in (0, T], \tag{3.24}$$

where the stiff constant coefficient linear term $Lu, L \in \mathbb{R}^{N\times N}$ and the nonlinear term $N(t,u)$ satisfy some forward Euler conditions, and the allowable time step for the forward Euler condition on the linear component can be significantly smaller than that for the nonlinear component. We first show that some forward Euler conditions on the linear term Lu indicate that $\mathrm{e}^{\tau L}u$ can preserve corresponding inequalities for any $\tau > 0$.

Lemma 3.5. *Assume that the linear term $Lu, u \in \mathbb{R}^N$ satisfies one or more of the following forward Euler conditions:*

$$\begin{aligned}
&\text{Strongstability}: && \|u+\tau Lu\| \le \|u\|, && \forall 0<\tau\le\bar{\tau}_{\mathrm{FE}},\ \forall u\in\mathbb{R}^N; && (3.25)\\
&\text{Positivity}: && u+\tau Lu \ge 0, && \forall 0<\tau\le\bar{\tau}_{\mathrm{FE}},\ \forall u\ge 0; && (3.26)\\
&\text{Rangeboundedness}: && m\le u+\tau Lu\le M, && \forall 0<\tau\le\bar{\tau}_{\mathrm{FE}},\ \forall m\le u\le M; && (3.27)\\
&\text{Maximumprinciple}: && \|u+\tau Lu\|_{l^\infty}\le\|u\|_{l^\infty}, && \forall 0<\tau\le\bar{\tau}_{\mathrm{FE}},\ \forall u\in\mathbb{R}^N; && (3.28)\\
&\text{Contractivity}: && \|u+\tau Lu\|\le\|u\|, && \forall 0<\tau\le\bar{\tau}_{\mathrm{FE}},\ \forall u\in\mathbb{R}^N. && (3.29)
\end{aligned}$$

Then, it holds that

$$\begin{aligned}
&\text{Strongstability}: && \|\mathrm{e}^{\tau L}u\|\le\|u\|, && \forall\tau>0,\ \forall u\in\mathbb{R}^N; && (3.30)\\
&\text{Positivity}: && \mathrm{e}^{\tau L}u\ge 0, && \forall\tau>0,\ \forall u\ge 0; && (3.31)\\
&\text{Rangeboundedness}: && m\le\mathrm{e}^{\tau L}u\le M, && \forall\tau>0,\ \forall m\le u\le M; && (3.32)\\
&\text{Maximumprinciple}: && \|\mathrm{e}^{\tau L}u\|_{l^\infty}\le\|u\|_{l^\infty}, && \forall\tau>0,\ \forall u\in\mathbb{R}^N; && (3.33)\\
&\text{Contractivity}: && \|\mathrm{e}^{\tau L}u\|\le\|u\|, && \forall\tau>0,\ \forall u\in\mathbb{R}^N; && (3.34)
\end{aligned}$$

where the inequalities in (3.26), (3.27), (3.31) and (3.32) are component-wise.

Proof. The proof for the preservation of strong stability (3.30) has been presented in Theorem 1 of [34]. Here, we consider the preservation of positivity as an example.

Assume $r > 0$. Note that $\mathrm{e}^z = \mathrm{e}^{-r}\mathrm{e}^{r+z} = \mathrm{e}^{-r}\sum_{k=0}^{\infty}\frac{r^k}{k!}\left(1+\frac{z}{r}\right)^k$. Let $\gamma_k = \frac{r^k}{k!}\mathrm{e}^{-r} > 0$, it holds that $\sum_{k=0}^{\infty}\gamma_k = 1$. Let I be the identity matrix in $\mathbb{R}^{N\times N}$. We show that $\mathrm{e}^{\tau L}u$ can be written as a convex combination of forward Euler steps with time-step size $\frac{\tau}{r}$, that is

$$\mathrm{e}^{\tau L}u = \sum_{k=0}^{\infty}\gamma_k\left(I+\frac{\tau}{r}L\right)^k u \ge 0, \quad \forall 0<\tau\le r\bar{\tau}_{\mathrm{FE}},\ \ \forall u\ge 0.$$

Since r can be arbitrarily large and $u \ge 0$, we have $\mathrm{e}^{\tau L}u \ge 0, \forall\tau > 0$.

Other results can be proved in the similar way. □

Remark 3.6. When considering the maximum principle, we point out that the forward Euler condition (3.28) is equivalent to the contraction semi-group property in Assumption 1.1. A proof of the equivalence is provided in Appendix B.

Then we take the maximum principle as an example to show the forward Euler condition on the sum of Lu and $N(t,u)$.

Lemma 3.7. *Assume $N(t,u)$ and Lu satisfy the forward Euler conditions (1.9) and (3.28), respectively. Then $Lu + N(t,u)$ satisfies the following condition,*

$$\|u+\tau[Lu+N(t,u)]\|_{l^\infty}\le\beta, \quad \forall 0<\tau\le\tau_{\mathrm{FE}} = \frac{\tilde{\tau}_{\mathrm{FE}}\bar{\tau}_{\mathrm{FE}}}{\tilde{\tau}_{\mathrm{FE}}+\bar{\tau}_{\mathrm{FE}}}, \quad \forall\|u\|_{l^\infty}\le\beta. \tag{3.35}$$

Proof. Let $\tilde{\kappa} = \frac{1}{\tau} \geq \frac{1}{\tilde{\tau}_{\mathrm{FE}}}$, $\bar{\kappa} = \frac{1}{\tau} \geq \frac{1}{\bar{\tau}_{\mathrm{FE}}}$. By multiplying (1.9) and (3.28) with $\tilde{\kappa}$ and $\bar{\kappa}$, respectively, we obtain

$$\|\tilde{\kappa}u + N(t,u)\|_{l^\infty} \leq \tilde{\kappa}\beta, \qquad \forall \tilde{\kappa} \geq \frac{1}{\tilde{\tau}_{\mathrm{FE}}}, \quad \forall \|u\|_{l^\infty} \leq \beta$$

$$\|\bar{\kappa}u + Lu\|_{l^\infty} \leq \bar{\kappa}\|u\|_{l^\infty} \leq \bar{\kappa}\beta, \quad \forall \bar{\kappa} \geq \frac{1}{\bar{\tau}_{\mathrm{FE}}}, \quad \forall \|u\|_{l^\infty} \leq \beta.$$

Then we obtain

$$\|(\tilde{\kappa} + \bar{\kappa})u + Lu + N(t,u)\|_{l^\infty} \leq (\tilde{\kappa} + \bar{\kappa})\beta, \quad \forall \tilde{\kappa} + \bar{\kappa} \geq \frac{1}{\tilde{\tau}_{\mathrm{FE}}} + \frac{1}{\bar{\tau}_{\mathrm{FE}}}, \quad \forall \|u\|_{l^\infty} \leq \beta,$$

which is equivalent to

$$\|u + \tau[Lu + N(t,u)]\|_{l^\infty} \leq \beta, \quad \forall 0 < \tau \leq \tau_{\mathrm{FE}} = \frac{\tilde{\tau}_{\mathrm{FE}}\bar{\tau}_{\mathrm{FE}}}{\tilde{\tau}_{\mathrm{FE}} + \bar{\tau}_{\mathrm{FE}}}, \quad \forall \|u\|_{l^\infty} \leq \beta.$$

□

By using Lemma 3.7 and Theorem 3.3, we present the following corollary without proof:

Corollary 3.8. *For the system (3.24), assume Lu satisfies one or more conditions in (3.25)–(3.29), and $N(t,u)$ satisfies corresponding forward Euler conditions with maximum allowable time step $\tilde{\tau}_{\mathrm{FE}}$. If pRK has non-negative Shu–Osher coefficients: $\alpha_{i,j} \geq 0, \beta_{i,j} \geq 0, i = 1,\ldots,s;\ j = 0,\ldots,i-1$ and SSP coefficient $\mathcal{C}$, let $f(t,u) := Lu + N(t,u)$, for any $\tau > 0$ if*

$$\kappa \geq \max\left\{\frac{1}{\tau_{\mathrm{FE}}} - \frac{\mathcal{C}}{\tau}, 0\right\}, \quad \text{where } \tau_{\mathrm{FE}} = \frac{\tilde{\tau}_{\mathrm{FE}}\bar{\tau}_{\mathrm{FE}}}{\tilde{\tau}_{\mathrm{FE}} + \bar{\tau}_{\mathrm{FE}}},$$

then pRK preserves the corresponding inequalities in Definitions 1.1–1.4.

Note that the strong stiffness of the linear term usually forces the forward Euler time-step size $\bar{\tau}_{\mathrm{FE}}$ to be small; thus, a large stabilization parameter κ will be needed to ensure the inequality-preserving properties. To reduce truncation errors introduced by a large κ, we consider taking advantage of properties of the operator $\mathrm{e}^{\tau L}$ in (3.30)–(3.34).

By treating e^{-tL} as the integrating factor, the SSP integrating factor approach for (3.24) has been extensively studied by Isherwood *et al.* [34–36]. Their studies showed that by applying the contraction semi-group property $\|\mathrm{e}^{\tau L}u\| \leq \|u\|$, the integrating factor approach only required the time step to satisfy the forward Euler condition on the nonlinear term for preserving strong stability, *i.e.*, $\tau \leq \mathcal{C}\tilde{\tau}_{\mathrm{FE}}$, which greatly relaxed the requirements $\tau \leq \mathcal{C}\frac{\tilde{\tau}_{\mathrm{FE}}\bar{\tau}_{\mathrm{FE}}}{\tilde{\tau}_{\mathrm{FE}}+\bar{\tau}_{\mathrm{FE}}}$ on explicit SSP schemes.

By incorporating the integrating factor method (integrating factor being e^{-tL}) to (3.24) with underlying parametric single-step schemes pRK (3.9), we obtain

$$u_{n,i} = \sum_{j=0}^{i-1} \mathrm{e}^{(c_i - c_j)\tau L}[\hat{\alpha}_{i,j}(\tau\kappa)u_{n,j} + \tau\hat{\beta}_{i,j}(\tau\kappa)N(t_{n,j}, u_{n,j})], \quad i = 1,\ldots,s.$$

Then substituting the corresponding definitions of $\hat{\alpha}_{i,j}(\tau\kappa)$ and $\hat{\beta}_{i,j}(\tau\kappa)$ (3.10) gives the following parametric integrating factor RK schemes:

$$\text{pIFRK}: u_{n,i} = \frac{1}{\psi_i(\tau\kappa)} \sum_{j=0}^{i-1} \psi_j(\tau\kappa)\mathrm{e}^{(c_i - c_j)\tau L}\left(\alpha_{i,j}u_{n,j} + \tau\beta_{i,j}\left[N(t_{n,j}, u_{n,j}) + \kappa u_{n,j}\right]\right), \quad i = 1,\ldots,s. \tag{3.36}$$

Although pIFRK may not preserve fixed points of (3.1) because of the introduction of the integrating factor, as compensation, we have the preservation of inequalities with smaller κ for pIFRK.

Theorem 3.9. *For the system (3.24), assume Lu satisfies one or more conditions in (3.25)–(3.29), and $N(t,u)$ satisfies corresponding forward Euler conditions with maximum allowable time step size $\tilde{\tau}_{\mathrm{FE}}$. If underlying RK satisfies*

(1) *Shu–Osher coefficients are non-negative:* $\alpha_{i,j} \geq 0,\ \beta_{i,j} \geq 0,\ i = 1, \ldots, s;\ j = 0, \ldots, i-1;$
(2) *Abscissas are non-decreasing:* $0 = c_0 \leq c_1 \leq c_2 \leq \ldots \leq c_s = 1;$

and has the SSP coefficient $\mathcal{C} \geq 0$*, then for any* $\tau > 0$*, if* $\kappa \geq \max\left\{\frac{1}{\tilde{\tau}_{\mathrm{FE}}} - \frac{\mathcal{C}}{\tau}, 0\right\}$*, the pIFRK method (3.36) preserves the corresponding inequalities in Definitions 1.1–1.4.*

Proof. Consider the preservation of strong stability as an example. We prove this by induction. Assuming that $\|u_{n,j}\| \leq \|u^n\|,\ j = 0, \ldots, i-1$, noting that $\frac{\tau\beta_{i,j}}{\alpha_{i,j}+\tau\kappa\beta_{i,j}} \leq \tilde{\tau}_{\mathrm{FE}}$, by applying the forward Euler condition on $N(t,u)$, the contraction semi-group of L (3.30) and definitions of $\psi_i(\tau\kappa) \geq 0,\ \forall \tau\kappa \geq 0$, we can derive

$$
\begin{aligned}
\|u_{n,i}\| &\leq \frac{1}{\psi_i(\tau\kappa)} \sum_{j=0}^{i-1} \psi_j(\tau\kappa)\left(\alpha_{i,j} + \tau\kappa\beta_{i,j}\right) \left\| \mathrm{e}^{(c_i - c_j)\tau L} \left[u_{n,j} + \frac{\tau\beta_{i,j}}{\alpha_{i,j} + \tau\kappa\beta_{i,j}} N(t_{n,j}, u_{n,j}) \right] \right\| \\
&\leq \frac{1}{\psi_i(\tau\kappa)} \sum_{j=0}^{i-1} \psi_j(\tau\kappa)(\alpha_{i,j} + \tau\kappa\beta_{i,j}) \left\| u_{n,j} + \frac{\tau\beta_{i,j}}{\alpha_{i,j} + \tau\kappa\beta_{i,j}} N(t_{n,j}, u_{n,j}) \right\| \\
&\leq \frac{1}{\psi_i(\tau\kappa)} \sum_{j=0}^{i-1} \psi_j(\tau\kappa)(\alpha_{i,j} + \tau\kappa\beta_{i,j}) \|u_{n,j}\| \\
&\leq \|u^n\|, \quad i \leq s.
\end{aligned}
$$

This completes the proof. □

In Theorem 3.9, a critical restriction on underlying RK schemes is the non-decreasing abscissas. Such explicit SSP RK schemes have been studied by Isherwood *et al.* [34], and shown to be at most fourth-order. We present some third- and fourth-order SSP RK schemes with non-decreasing abscissas (denoted by a superscript "+") and optimal SSP coefficients (w.r.t. the stage number) below. We mention that, when $\kappa = 0$, the pIFRK schemes reduce to the IFRK schemes developed in [34].

$\mathrm{RK}^+(3,3)$ [34], $\mathcal{C} = \frac{3}{4}$, $c = \left[0, \frac{2}{3}, \frac{2}{3}\right]^T$:

$$
\begin{cases}
u_{n,1} = u_{n,0} + \dfrac{2}{3}\tau f(t_{n,0}, u_{n,0}), \\
u_{n,2} = \dfrac{2}{3}u_{n,0} + \dfrac{1}{3}\left[u_{n,1} + \dfrac{4}{3}\tau f(t_{n,1}, u_{n,1})\right], \\
u_{n,3} = \dfrac{59}{128}u_{n,0} + \dfrac{15}{128}\left[u_{n,0} + \dfrac{4}{3}\tau f(t_{n,0}, u_{n,0})\right] + \dfrac{27}{64}\left[u_{n,2} + \dfrac{4}{3}\tau f(t_{n,2}, u_{n,2})\right].
\end{cases}
$$

$\mathrm{RK}^+(5,4)$ [34], $\mathcal{C} \approx 1.346586417284006$, $c \approx [0, 0.4549, 0.5165, 0.5165, 0.9903]^T$:

$$
\begin{cases}
u_{n,1} = 0.387392167970373u_{n,0} + 0.612607832029627\left[u_{n,0} + \dfrac{\tau}{\mathcal{C}} f(t_{n,0}, u_{n,0})\right], \\
u_{n,2} = 0.568702484115635u_{n,0} + 0.431297515884365\left[u_{n,1} + \dfrac{\tau}{\mathcal{C}} f(t_{n,1}, u_{n,1})\right], \\
u_{n,3} = 0.589791736452092u_{n,0} + 0.410208263547908\left[u_{n,2} + \dfrac{\tau}{\mathcal{C}} f(t_{n,2}, u_{n,2})\right], \\
u_{n,4} = 0.213474206786188u_{n,0} + 0.786525793213812\left[u_{n,3} + \dfrac{\tau}{\mathcal{C}} f(t_{n,3}, u_{n,3})\right], \\
u^{n+1} = 0.270147144537063u_{n,0} + 0.029337521506634\left[u_{n,0} + \dfrac{\tau}{\mathcal{C}} f(t_{n,0}, u_{n,0})\right] \\
\qquad + 0.239419175840559\left[u_{n,1} + \dfrac{\tau}{\mathcal{C}} f(t_{n,1}, u_{n,1})\right] + 0.227000995504038\left[u_{n,3} + \dfrac{\tau}{\mathcal{C}} f(t_{n,3}, u_{n,3})\right] \\
\qquad + 0.234095162611706\left[u_{n,4} + \dfrac{\tau}{\mathcal{C}} f(t_{n,4}, u_{n,4})\right].
\end{cases}
\tag{3.37}
$$

3.3. Inequality-preserving exponential time difference schemes

Noting that the existing higher-than-first-order unconditionally SSP [3, 23–25] and positivity-preserving [26, 28] integrators mentioned in the introduction are specifically designed for particular problems, and have not been proven to preserve inequality structures for general problems. For comparison, we present the well-known ETD integrators in this section. Ostermann and co-authors [77, 78] proved that the order of positive ETD Runge–Kutta and multi-step schemes cannot exceed two. Therefore, we only show that the ETD1 and ETD2 schemes preserve inequality structures for any time step size by adopting a stabilization technique.

To briefly illustrate the ETD schemes, we introduce the functions [79]

$$\varphi_k(z) = \int_0^1 \mathrm{e}^{(1-s)z} \frac{s^{k-1}}{(k-1)!} \mathrm{d}s > 0, \quad k \geq 1, \tag{3.38}$$

which satisfy the recursion

$$\varphi_k(z) = \frac{\varphi_{k-1}(z) - \frac{1}{(k-1)!}}{z}, \quad \varphi_0(z) = \mathrm{e}^z. \tag{3.39}$$

Consider the first- and second-order explicit ETD schemes [74, 79] with Butcher-like tableaux

$$\begin{array}{c|ccc} \vdots & \cdots & \cdots & \cdots \\ c_i & \cdots & a_{i,j}(z) & \cdots \\ \vdots & \cdots & \cdots & \cdots \\ \hline 1 & \cdots & a_{s,j}(z) & \cdots \end{array} = \quad \text{ETD1: } \begin{array}{c|c} 0 & 0 \\ \hline 1 & \varphi_1 \end{array}, \qquad \text{ETD2: } \begin{array}{c|cc} 0 & 0 & \\ 1 & \varphi_1 & 0 \\ \hline 1 & \varphi_1 - \varphi_2 & \varphi_2 \end{array}. \tag{3.40}$$

By introducing $\kappa(u-u)$ to (3.24), we obtain

$$u_t = Lu - \kappa u + N(t,u) + \kappa u =: L_\kappa u + N_\kappa(t,u), \tag{3.41}$$

where $L_\kappa := L - \kappa I$, $N_\kappa(t,u) := N(t,u) + \kappa u$. Taking the stiff matrix L_κ as the variable of φ_j functions in (3.40), we obtain the stabilization ETD1/2 schemes in a unified framework

$$u_{n,i} = \varphi_0(\tau L_\kappa)u^n + \tau \sum_{j=0}^{i-1} a_{i,j}(\tau L_\kappa) N_\kappa(t_{n,j}, u_{n,j}), \quad i = 1, \ldots, s. \tag{3.42}$$

Below, we take the strong stability as an example to show that ETD1/2 preserve inequality structures when κ is suitably chosen. Here and after, Lu and $N(t,u)$ are assumed to satisfy the forward Euler conditions (3.25) and (1.2) on strong stability with maximum time-step sizes $\bar{\tau}_{\mathrm{FE}}$ and $\tilde{\tau}_{\mathrm{FE}}$, respectively. We first present some useful lemmas.

When $k = 1$, the recursion relationship (3.39) yields the following Lemma.

Lemma 3.10. *For any $z \neq 0$, it holds that $\varphi_0(z) - z\varphi_1(z) = 1$.*

Lemma 3.11. *For any $\kappa > 0$ and $\tau > 0$, it holds that*

(1) $\|\varphi_k(\tau L_\kappa)u\| \leq \varphi_k(-\tau\kappa)\|u\|, \ k \geq 1.$
(2) $\|[\varphi_1(\tau L_\kappa) - \varphi_2(\tau L_\kappa)]u\| \leq [\varphi_1(-\tau\kappa) - \varphi_2(-\tau\kappa)]\,\|u\|.$

Proof. By using the definitions of $\varphi_k(\tau L_\kappa)$ and the inequality (3.30), we derive

$$\begin{aligned}
\|\varphi_k(\tau L_\kappa)u\| &= \left\| \frac{1}{\tau^k}\int_0^\tau \mathrm{e}^{(\tau-s)L_\kappa} u \frac{s^{k-1}}{(k-1)!}\mathrm{d}s \right\| \\
&\le \frac{1}{\tau^k}\int_0^\tau \mathrm{e}^{-(\tau-s)\kappa} \left\| \mathrm{e}^{(\tau-s)L} u \right\| \frac{s^{k-1}}{(k-1)!}\mathrm{d}s \\
&\le \frac{1}{\tau^k}\int_0^\tau \mathrm{e}^{-(\tau-s)\kappa} \frac{s^{k-1}}{(k-1)!}\mathrm{d}s \|u\| \\
&= \varphi_k(-\tau\kappa)\|u\|, \quad \forall k \ge 1.
\end{aligned}$$

$$\begin{aligned}
\|[\varphi_1(\tau L_\kappa) - \varphi_2(\tau L_\kappa)]\, u\| &= \left\| \frac{1}{\tau}\int_0^\tau \left(1-\frac{s}{\tau}\right) \mathrm{e}^{(\tau-s)L_\kappa} u \mathrm{d}s \right\| \\
&\le \frac{1}{\tau}\int_0^\tau \left(1-\frac{s}{\tau}\right) \mathrm{e}^{-(\tau-s)\kappa} \left\| \mathrm{e}^{(\tau-s)L} u \right\| \mathrm{d}s \\
&\le \frac{1}{\tau}\int_0^\tau \left(1-\frac{s}{\tau}\right) \mathrm{e}^{-(\tau-s)\kappa} \mathrm{d}s \|u\| \\
&= [\varphi_1(-\tau\kappa) - \varphi_2(-\tau\kappa)]\|u\|.
\end{aligned}$$

This completes the proof. □

Theorem 3.12. *For the system (3.24), assume Lu satisfies one or more conditions in (3.25)–(3.29), and $N(t,u)$ satisfies corresponding forward Euler conditions with maximum allowable time step size $\tilde{\tau}_{\mathrm{FE}}$. If $\kappa \ge \frac{1}{\tilde{\tau}_{\mathrm{FE}}}$, the ETD1/2 schemes preserve the corresponding inequalities in Definitions 1.1–1.4 for any $\tau > 0$.*

Proof. Consider the preservation of strong stability. We prove this by induction.

Note that the forward Euler condition on $N(t,u)$ is equivalent to the circle condition

$$\|\kappa u + N(t,u)\| \le \kappa\|u\|, \quad \forall \kappa \ge \frac{1}{\tilde{\tau}_{\mathrm{FE}}}. \tag{3.43}$$

For the ETD1 and ETD2 Butcher tableaux in (3.40), we can derive

$$\sum_{j=0}^{i-1} a_{i,j}(-\tau\kappa) = \varphi_1(-\tau\kappa), \quad i = 1,\dots,s. \tag{3.44}$$

Assuming that $\|u_{n,j}\| \le \|u^n\|$, $j = 0,1,\dots,i-1$, since every $a_{i,j}(\tau L_\kappa)$ of the Butcher tableaux (3.40) consists of the functions $\varphi_i(\tau L_\kappa), i = 1,2$, and $\varphi_1(\tau L_\kappa) - \varphi_2(\tau L_\kappa)$, by using Lemmas 3.11 and 3.10, the inequality (3.43), and the equality (3.44), we obtain

$$\begin{aligned}
\|u_{n,i}\| &\le \|\varphi_0(\tau L_\kappa)u^n\| + \tau\sum_{j=0}^{i-1}\|a_{i,j}(\tau L_\kappa)N_\kappa(t_{n,j},u_{n,j})\| \\
&\le \left[\varphi_0(-\tau\kappa) + \tau\kappa\sum_{j=0}^{i-1} a_{i,j}(-\tau\kappa)\right]\|u^n\| \\
&= [\varphi_0(-\tau\kappa) + \tau\kappa\varphi_1(-\tau\kappa)]\,\|u^n\| \\
&= \|u^n\|, \quad i \le s.
\end{aligned}$$

Thus $\left\|u^{n+1}\right\| = \|u_{n,s}\| \le \|u^n\|$. The proofs for preservation of other structures in Definitions 1.2–1.4 can be performed similarly. □

Remark 3.13. The preservation of maximum principles for Allen–Cahn-type parabolic equations using stabilization ETD1/2 has been proven by Du *et al.* [4,38]. The results there demonstrate the efficiency and stability of stabilization methods. When considering the system (1.1), the corresponding stabilization ETD1/2 schemes have the form

$$u_{n,i} = \varphi_0(-c_i\tau\kappa)u^n + \tau\sum_{j=0}^{i-1} a_{i,j}(-\tau\kappa)[f(t_{n,j}, u_{n,j}) + \kappa u_{n,j}], \quad i = 1, \dots, s.$$

Since the proof of inequality-preservation can be similarly carried out as Theorem 3.12 when $\kappa \geq \frac{1}{\tau_{\mathrm{FE}}}$ for any $\tau > 0$, we omit the details here. Because of the introduced stabilization parameter, the time inconsistency of ETD1/2 also exists. This issue will be illustrated in the numerical experiments.

4. Numerical analysis

4.1. Linear stability analysis

Theorems 3.3 and 3.9 show that proposed pRK and pIFRK are inequality-preserving for nonlinear systems (1.1) and (3.24), respectively. In this section, we carry out linear stability analysis for pRK schemes.

Consider a linear test equation [57,66]

$$u_t = \lambda u = (1-\alpha)\lambda u + \alpha\lambda u. \tag{4.1}$$

Let $\kappa = -\alpha\lambda$ be the stabilization parameter. Applying an s-stage, pth-order ($p = s, s \leq 4$) explicit pRK scheme (3.8)–(4.1) yields

$$u_{n,i} = \frac{1}{\psi_i(-\alpha\tau\lambda)}\sum_{j=0}^{i-1}\psi_j(-\alpha\tau\lambda)[\alpha_{i,j}u_{n,j} + \tau\beta_{i,j}(1-\alpha)\lambda u_{n,j}], \quad i = 1, \dots, s. \tag{4.2}$$

Lemma 4.1. *The solution of an s-stage pRK scheme to (4.1) is given by* $u^{n+1} = \frac{\psi_s((1-\alpha)\tau\lambda)}{\psi_s(-\alpha\tau\lambda)}u_{n,0}$.

Proof. We prove this by mathematical induction. The first stage solution is calculated by

$$u_{n,1} = \frac{1}{\psi_1(-\alpha\tau\lambda)}\psi_0(-\alpha\tau\lambda)\left[\alpha_{1,0}u_{n,0} + \tau\beta_{1,0}(1-\alpha)\lambda u_{n,0}\right] = \frac{\psi_1\left((1-\alpha)\tau\lambda\right)}{\psi_1(-\alpha\tau\lambda)}u_{n,0}.$$

Assuming that $u_{n,j} = \frac{\psi_j((1-\alpha)\tau\lambda)}{\psi_j(-\alpha\tau\lambda)}u_{n,0}$, $j = 0, \dots, i-1$, by using definitions of $\psi_i(z)$ and the formulation (4.2), we obtain

$$\begin{aligned} u_{n,i} &= \frac{1}{\psi_i(-\alpha\tau\lambda)}\sum_{j=0}^{i-1}\psi_j\left((1-\alpha)\tau\lambda\right)\left[\alpha_{i,j} + \tau\beta_{i,j}(1-\alpha)\lambda\right]u_{n,0} \\ &= \frac{\psi_i\big((1-\alpha)\tau\lambda\big)}{\psi_i(-\alpha\tau\lambda)}u_{n,0}, \quad i \leq s. \end{aligned}$$

Thus $u^{n+1} = u_{n,s} = \frac{\psi_s((1-\alpha)\tau\lambda)}{\psi_s(-\alpha\tau\lambda)}u_{n,0}$. □

Denote $z = \tau\lambda$, and apply the order conditions in Table 1, we calculate the stability function of the pRK formulation (4.2) as

$$R_s(\alpha, z) = \frac{\psi_s\left((1-\alpha)z\right)}{\psi_s(-\alpha z)} = \frac{\sum_{k=0}^{s}\frac{((1-\alpha)z)^k}{k!}}{\sum_{k=0}^{s}\frac{(-\alpha z)^k}{k!}}, \quad s \leq 4. \tag{4.3}$$

Recall [67,80] that some stability properties for a method with the general stability function $R(z)$ are defined as follows:

- A method is called A-stable if $|R(z)| \leq 1$ for all $\mathrm{Re}(z) \leq 0$;
- A method is called L-stable if it is A-stable and $\lim_{z\to\infty} |R(z)| = 0$;
- A method is called Strongly A-stable [80, 81] if it is A-stable and $\lim_{z\to\infty} |R(z)| = \mu < 1$;
- A method is called nearly A-stable/L-stable/Strongly A-stable [67] if the stability region contains the whole left-half complex plane except small regions around the imaginary axis.

To analyze the stability of proposed schemes, we present a useful lemma.

Lemma 4.2 (A-stability from the maximum modulus principle, p. 43 in [82])**.** *A method with stability function $R(z)$ is A-stable if and only if*

(1) *$R(z)$ is analytic in the left-half complex plane $\mathbb{C}^-$;*
(2) *$|R(i\sigma)| \leq 1$ for all real values of σ.*

Then a property of proposed schemes (4.2) is given as follows:

Lemma 4.3. *The s-stage, pth order ($p = s \leq 4$) pRK schemes with $\alpha = \frac{1}{2}$ are A-stable.*

Proof. We show that $|R_s\left(\frac{1}{2}, z\right)| \leq 1, \forall \mathrm{Re}(z) \leq 0,\ s = 1, \ldots, 4$.

Let $\phi_s(z) = \sum_{k=0}^{s} \frac{z^k}{k!}, s \geq 1$. Since $R_s\left(\frac{1}{2}, z\right) = \frac{\phi_s\left(\frac{1}{2}z\right)}{\phi_s\left(-\frac{1}{2}z\right)}$, it follows by symmetry that $\left|R_s\left(\frac{1}{2}, \mathrm{i}\sigma\right)\right| = 1$ for all real σ. Using the fact that the roots z_i of the polynomial $\phi_s(-z), s \leq 4$ satisfy $\mathrm{Re}(z_i) > 0,\ i = 1, \ldots, s$. Then $R_s\left(\frac{1}{2}, z\right)$ is analytic in $\mathbb{C}^-$. Next, it is obvious that $\lim_{z\to\infty} \left|R_s\left(\frac{1}{2}, z\right)\right| = 1$. By using Lemma 4.2, we have $\left|R_s\left(\frac{1}{2}, z\right)\right| \leq 1,\ s = 1 - -4$, for all $\mathrm{Re}(z) \leq 0$. □

As α increases from 0 to 1.25, we obtain the boundaries of the stability regions for the proposed pRK schemes as $|R_s(\alpha, z)| = 1$. The stability boundary curves for some pRK schemes are presented in Figure 1. Clearly, we observe that for each scheme, the stability region becomes larger as α increases. When α equals zero, the stability regions of pRK reduce to those of classical RK schemes. For $s = 1,\ 2$, when $\alpha \geq \frac{1}{2}$, the stability regions contain the whole left-half complex plane, see Figure 1(a) and (e). For $s = 3$–5, when $\alpha > \frac{1}{2}$, the stability regions exclude part of the left-half complex plain, see Figure 1(f, g, d, h). We remark that a larger α may increase the stability but reduce the accuracy, as noted by Ju *et al.* [62] for stabilization integrating factor methods.

By simple calculation, we obtain

$$\lim_{z\to\infty} |R_s(1, z)| = \lim_{z\to\infty} \left|\frac{1}{\phi_s(-z)}\right| = 0,$$
$$\lim_{z\to\infty} |R_s(\alpha, z)| = \left|\frac{1-\alpha}{\alpha}\right|^s < 1, \quad \forall \alpha > \frac{1}{2}.$$

From the above analysis, we draw the following conclusion about the proposed pRK schemes:

Corollary 4.4. *The pRK schemes for (4.1) have the following properties:*

(1) *pRK(1, 1) and pRK(2, 2) are A-stable when $\alpha \geq \frac{1}{2}$; L-stable when $\alpha = 1$; strongly A-stable for all $\alpha > \frac{1}{2}$;*
(2) *pRK(3, 3) and pRK(4, 4) are A-stable when $\alpha = \frac{1}{2}$; nearly L-stable when $\alpha = 1$; and nearly, strongly A-stable for all $\alpha > \frac{1}{2}$.*

Remark 4.5. For other pRK schemes with $s > p$, the roots of polynomial $\psi_s(-z)$ may lie on the left-half complex plain, then the stability function $R_s(\alpha, z)$ may not be analytic in $\mathbb{C}^-$. Thus the results in Corollary 4.4 may not hold for $s > p$. However, for pRK(5, 4) [underlying scheme (3.23)] with $\psi_5(-z) \approx -0.0044777z^5 + \frac{1}{24}z^4 - \frac{1}{6}z^3 + \frac{1}{2}z^2 - z + 1$, and pRK$^+$(5, 4) [underlying scheme (3.37)] with $\psi_5(-z) \approx -0.0045071z^5 + \frac{1}{24}z^4 - \frac{1}{6}z^3 + \frac{1}{2}z^2 - z + 1$, the stability functions $R_5(\alpha, z)$ are analytic in $\mathbb{C}^-$, thus Lemma 4.3 and the second part of Corollary 4.4 still hold, see Figure 1(d) and (h).

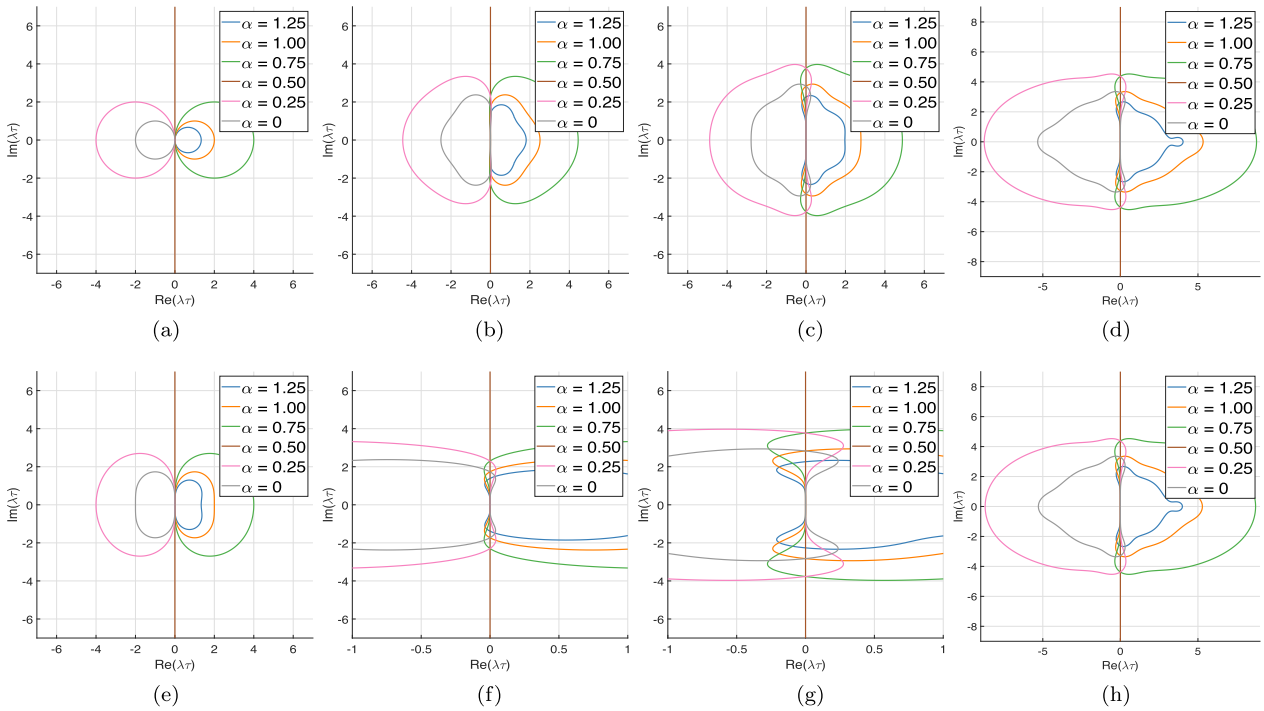

FIGURE 1. Boundaries of stability regions for pRK(s, p) with different values of α. (a) pRK(1, 1), (b) pRK(3, 3), (c) pRK(4, 4), (d) pRK(5, 4) (3.23), (e) pRK(2, 2), (f) pRK(3, 3) zoom-in, (g) pRK(4, 4) zoom-in, and (h) pRK$^+$(5, 4) (3.37).

4.2. Error estimate

In this section, we carry out a rigorous error analysis for the proposed pRK schemes.

Theorem 4.6. *Assume (1.1) has an exact solution $u(t) \in C^{p+1}\left([0,T];\mathbb{R}^N\right)$, and u^n is computed by an s-stage, pth-order ($p \le 4$) pRK scheme that has non-negative underlying Shu–Osher coefficients. Assuming $f(t,u)$ meets one condition in (1.2)–(1.6), the corresponding Lipschitz condition in (2.1)–(2.5) also holds, and $\kappa \ge \frac{1}{\tau_{\mathrm{FE}}}$, then we have the following error estimate for pRK schemes:*

$$\|u(t_n) - u^n\|_* \le C\left(\mathrm{e}^{(K+\kappa)st_n} - 1\right)\tau^p, \quad \text{for } t_n \le T,$$

where the constant $C > 0$ depends on the stage number s, the Lipschitz constant K, the stabilization parameter κ, the $C^{p+1}\left([0,T];\mathbb{R}^N\right)$ norm of u, but is independent of τ.

Proof. Let us take the convergence of SSP pRK schemes in Definition 1.1 as an example. Assume that $f(t,u)$ satisfies the forward Euler condition (1.2) and the Lipschitz condition (2.1). Denote $f_\kappa(t,u) = f(t,u) + \kappa u$. Notice that the Shu–Osher modification (3.8) is equivalent to the Butcher modification (3.12), we introduce reference functions [83, 84] $U_{n,i}$ for $0 \le i \le s$, with $U_{n,0} = u(t_n)$ and $U_{n,s} = u(t_{n+1})$ based on the Butcher

modification

$$
\begin{aligned}
U_{n,i} &= \frac{1}{\psi_i(\tau\kappa)}\left[u(t_n)+\tau\sum_{j=0}^{i-1}a_{i,j}\psi_j(\tau\kappa)f_\kappa(t_{n,j},U_{n,j})\right], \quad i=1,\dots,s-1,\\
U_{n,s} &= \frac{1}{\psi_s(\tau\kappa)}\left[u(t_n)+\tau\sum_{j=0}^{s-1}a_{s,j}\psi_j(\tau\kappa)f_\kappa(t_{n,j},U_{n,j})\right]+R_s^n.
\end{aligned}
\tag{4.4}
$$

For an s-stage, pth-order ($p\le 4$) underlying pRK scheme, Lemma 3.2 shows that the truncation errors satisfy

$$
\max_{0\le n\le\lfloor T/\tau\rfloor-1}\|R_s^n\|_*\le C_s\tau^{p+1},
$$

where C_s depends on s, κ, and the $C^{p+1}\left([0,T];\mathbb{R}^N\right)$-norm of u, but is independent of τ.

Let $e^n=u(t_n)-u^n$ and $e_{n,i}=U_{n,i}-u_{n,i}$ for $0\le i\le s$. Then $e_{n,0}=e^n$ and $e_{n,s}=e^{n+1}$. Subtracting (3.12) from (4.4) yields

$$
\begin{aligned}
e_{n,i} &= \frac{1}{\psi_i(\tau\kappa)}\left(e^n+\tau\sum_{j=0}^{i-1}a_{i,j}\psi_j(\tau\kappa)[f_\kappa(t_{n,j},U_{n,j})-f_\kappa(t_{n,j},u_{n,j})]\right), \quad i=1,\dots,s-1,\\
e_{n,s} &= \frac{1}{\psi_s(\tau\kappa)}\left(e^n+\tau\sum_{j=0}^{s-1}a_{s,j}\psi_j(\tau\kappa)[f_\kappa(t_{n,j},U_{n,j})-f_\kappa(t_{n,j},u_{n,j})]\right)+R_s^n.
\end{aligned}
$$

Since Theorem 3.3 guarantees that $\|u_{n,i}\|\le\|u^0\|$ and $\|U_{n,i}\|\le\|u^0\|$, $i=0,\dots,s$, we can use the Lipschitz condition (2.1) to obtain

$$
\|f_\kappa(t_{n,i},U_{n,i})-f_\kappa(t_{n,i},u_{n,i})\|_*\le(K+\kappa)\|e_{n,i}\|_*, \quad i=0,\dots,s.
$$

For underlying RK schemes with non-negative Shu–Osher coefficients and non-decreasing abscissas presented in this work, it can be verified that $0<\frac{1}{\psi_i(\tau\kappa)}\le 1$, $0\le\frac{a_{i,j}\psi_j(\tau\kappa)}{\psi_i(\tau\kappa)}\le 1, i=1,\dots,s, j<i$. Then, we derive

$$
\begin{aligned}
\|e_{n,i}\|_* &\le \frac{1}{\psi_i(\tau\kappa)}\left[\|e^n\|_*+\tau\sum_{j=0}^{i-1}a_{i,j}\psi_j(\tau\kappa)\,\|f_\kappa(t_{n,j},U_{n,j})-f_\kappa(t_{n,j},u_{n,j})\|_*\right]\\
&\le \|e^n\|_*+\tau(K+\kappa)\sum_{j=0}^{i-1}\|e_{n,j}\|_*\\
&\le (1+\tau(K+\kappa))^i\,\|e^n\|_*, \quad i=1,\dots,s-1,\\
\|e_{n,s}\|_* &\le \frac{1}{\psi_s(\tau\kappa)}\left[\|e^n\|_*+\tau\sum_{j=0}^{s-1}a_{s,j}\psi_j(\tau\kappa)\,\|f_\kappa(t_{n,j},U_{n,j})-f_\kappa(t_{n,j},u_{n,j})\|_*\right]+\|R_s^n\|_*\\
&\le \|e^n\|_*+\tau(K+\kappa)\sum_{j=0}^{s-1}\|e_{n,j}\|_*+C_s\tau^{p+1}\\
&\le (1+\tau(K+\kappa))^s\,\|e^n\|_*+C_s\tau^{p+1}.
\end{aligned}
$$

By induction, we obtain

$$
\begin{aligned}
\|e^n\|_* &\le (1+\tau(K+\kappa))^{sn}\,\|e^0\|_*+C_s\tau^{p+1}\sum_{i=0}^{n-1}(1+\tau(K+\kappa))^{si}\\
&\le (1+\tau(K+\kappa))^{sn}\,\|e^0\|_*+\frac{C_s}{(K+\kappa)}\left(\mathrm{e}^{(K+\kappa)sn\tau}-1\right)\tau^p.
\end{aligned}
$$

Let $C = \frac{C_s}{(K+\kappa)s}$, we obtain the desired result since $\|e^0\|_* = 0$ and $n\tau = t_n$.

The convergence of pRK schemes for (1.1) satisfying other conditions can be carried out similarly. □

5. Numerical experiments

In this section, we underline our theoretical analysis with numerical experiments. For the convenience of discussion, we consider the preservation of strong stability for linear advection equations and the maximum principle for AC-type semilinear parabolic equations. First, we test the proposed pRK and pIFRK schemes to verify the convergence. Then we study the inequality-preservation of proposed schemes in terms of their allowable stabilization parameter for a given time-step size τ. When adopting parametric integrating factor and ETD1/2 schemes, we compute the products of matrix exponentials with vectors via the fast Fourier transform to accelerate computations [38].

5.1. Convergence order verification

We study the convergence of the proposed pRK (3.9) and pIFRK (3.36) schemes on ODE systems obtained from spatial-discretizations of a linear advection equation (5.1) and a nonlinear AC equation (5.3), respectively.

Example 5.1. Consider the linear advection equation

$$\begin{cases} u_t + au_x = 0, \\ u(x,0) = \sin(2\pi x), \end{cases} \qquad \Omega = (0,1), \tag{5.1}$$

with periodic boundary conditions.

We set $a = 1$ and employ a standard first-order upwind finite difference method for the advection term to preserve the total variation (TV) of u, *i.e.*, $\|\boldsymbol{u}\| := \sum_j |u_{j+1} - u_j|$. Let N denote the number of space grid points, and the mesh size be $h = \frac{1}{N}\cdot$ Denote the set of grid points as $\Omega_h = \{x_j | x_j = jh,\ j = 0, 1, \ldots, N-1\}$. Let $\mathbb{V}_N = \{\boldsymbol{v} | \boldsymbol{v} = (v_j), x_j \in \Omega_h\} \subset \mathbb{R}^N$ be the space of grid functions defined on Ω_h. Denote the first-order upwind differentiation matrix by D. Then we obtain a linear system of ODEs: $\boldsymbol{u}_t = f(t, \boldsymbol{u}) := -aD\boldsymbol{u}$. The numerical errors are computed using

$$\text{Error}_{l^\infty} = \|\bar{\boldsymbol{u}}^n - \boldsymbol{u}^n\|_{l^\infty}, \tag{5.2}$$

where $\bar{\boldsymbol{u}}^n$ is the reference solution computed with a refined time-step size, and $\boldsymbol{u}^n$ is the numerical solution obtained by pRK, pIFRK or ETD1/2. For the temporal convergence, the grid number is set to $N = 256$, and the reference solution is computed with $\tau = 2^{-18}$ using the fourth-order RK(5, 4) scheme (3.23). The time-step size required by the forward Euler condition with respect to the total variation is $\tau \le \tau_{\text{FE}} = \frac{h}{|a|} = h\cdot$ Since the theoretical convergence orders are verified using a fixed value of κ, we choose the stabilization parameter $\kappa = \frac{1}{\tau_{\text{FE}}}$ that satisfies the requirement (3.20) for all time-step sizes.

Figure 2(a) presents the numerical errors for the linear advection equation (5.1) at $T = 1$ obtained by pRK schemes with underlying RK(1, 1), RK(2, 2), RK(3, 3), RK(4, 4), and RK(5, 4) Butcher tableaux in Section 3.1, and ETD1/2 in Section 3.3. Clearly, we observe that each of the proposed schemes converges with the theoretical order of accuracy. Although pRK(1, 1) and pRK(2, 2) are less accurate than ETD1 and ETD2, respectively, the numerical errors can be greatly reduced by using the high-order pRK(3, 3), pRK(4, 4) and pRK(5, 4) schemes. This shows the advantages of using high-order pRK schemes.

Example 5.2. Consider the AC equation

$$\begin{cases} u_t = \epsilon^2 \Delta u + u - u^3, \\ u(x,0) = 0.1\sin(2\pi x) + 0.05, \end{cases} \qquad \Omega = (0,2), \tag{5.3}$$

with periodic boundary conditions.

By discretizing the Laplace operator using the standard second-order central finite difference method, and denoting the obtained differentiation matrix by D_2, we obtain a semi-discrete system in the form $\boldsymbol{u}_t = L\boldsymbol{u}+N(\boldsymbol{u})$, where L is given by $\epsilon^2 D_2$, $N(\boldsymbol{u}) = \boldsymbol{u} - \boldsymbol{u}^3$, and the powers of vectors are component-wise. Since the central finite difference discretization of the Laplace operator in one-, two- and three-dimensional domains with periodic boundary conditions produces a diagonally dominant matrix with negative diagonal entries, it can be verified that L satisfies the condition that $\|\mathrm{e}^{\tau L}\|_\infty \leq 1$.

We set $\epsilon = 0.01$ and solve this problem to time $T = 2.0$. For the temporal convergence, the grid number is set to $N = 256$, and the reference solution in (5.2) is computed with $\tau = 2^{-12}$ using the fourth-order pIFRK$^+$(5, 4) scheme (3.37) with $\kappa = 0$. Note that $N(\boldsymbol{u})$ satisfies the forward Euler condition (1.9) for $\beta = 1$ and $\tilde{\tau}_{\mathrm{FE}} = \frac{1}{2}$ (Theo. 1 in [31]). Thus we take two different stabilization parameters, $\kappa = 1$ and $\kappa = \frac{1}{\tilde{\tau}_{\mathrm{FE}}} = 2$, to show the influence of the stabilization parameter.

The numerical errors (5.2) computed using ETD1/2, and pIFRK with underlying RK(1, 1), RK(2, 2), RK$^+$(3, 3), RK(4, 4) and RK$^+$(5, 4) are demonstrated in Figure 2(b) and (c). As expected, we observe perfect first- to fourth-order convergence in the time direction for corresponding schemes, and the numerical errors do not blow up at large time step $\tau = 1$. As κ increases from 1 to 2, the numerical errors become larger. Therefore, to reduce additional splitting errors, it is important to develop high-order schemes that can be used with small stabilization parameters.

5.2. Strong-stability-preserving tests

Example 5.3. We test the strong-stability preservation of the proposed schemes on a linear advection equation with discontinuous initial data

$$u_t + au_x + u_x = 0, \quad x \in (0,1),$$
$$u(x,0) = \begin{cases} 1, & x \in \left[\frac{1}{4}, \frac{3}{4}\right], \\ 0, & x \in \left[0, \frac{1}{4}\right) \cup \left(\frac{3}{4}, 1\right], \end{cases}$$

and periodic boundary conditions.

We denote the semi-discrete system obtained by the upwind scheme as $\boldsymbol{u}_t = L\boldsymbol{u}+N(\boldsymbol{u})$, where $L = -aD$ and $N(\boldsymbol{u}) = -D\boldsymbol{u}$. We set $N = 1000$, $\tilde{\tau}_{\mathrm{FE}} = \frac{1}{1000}$, $\kappa = \frac{1}{\tilde{\tau}_{\mathrm{FE}}}$ for ETD1/2, $\kappa = \max\left\{\frac{1}{\tilde{\tau}_{\mathrm{FE}}} - \frac{\mathcal{C}}{\tau}, 0\right\}$ for pIFRK, and solve this problem for 100 time steps using existing IFRK [34], ETD1/2, and the proposed pIFRK schemes (3.36). When $a = 0$, the IFRK and pIFRK schemes become the RK and pRK schemes, respectively. The results of the maximum rise in TV obtained by second- to fourth-order RK-type schemes with $a = 0, 5, 10$ are presented in Figure 3. It can be observed that the allowable time-step size of each IFRK scheme becomes larger as a increases. This is caused by the significant damping of exponential terms [34], thus reducing the oscillations and associated rise in total variation.

The results computed by pRK, pIFRK and ETD1/2 with the prescribed values of κ are noteworthy. As an improvement over the existing RK and IFRK schemes, we can clearly observe that all pRK, pIFRK and ETD1/2 schemes (dashed lines with markers in Fig. 3) preserve the strong stability for any value of τ by introducing the stabilizing parameter.

Next, we compare the solutions of pIFRK schemes with those obtained by IFRK schemes [34], the unconditionally SSP backward Euler (BE) scheme, and ETD1/2 schemes at large time steps. In Figure 4, we present solution profiles computed by different schemes with $a = 0.1$ at $T = 0.18$. In Figure 4(a), the time steps are chosen as BE, ETD1, ETD2, (p)IFRK(2, 2): $\tau = 0.00113$; (p)IFRK$^+$(3, 3): $\tau = 0.001355$; and (p)IFRK(4, 4): $\tau = 0.00151$. The corresponding ratios $\frac{\tau}{\tilde{\tau}_{\mathrm{FE}}}$ are: 1.13, 1.355, 1.51. Since the time steps are larger than $\mathcal{C}\tilde{\tau}_{\mathrm{FE}}$ for all IFRK schemes, oscillations appear in the solution profiles obtained by these schemes. With the introduction of stabilization parameters, ETD1/2 and pIFRK schemes produce stable profiles, and the time delays of pIFRK schemes are weaker than those of ETD1/2. Moreover, the solutions of pIFRK(2, 2) and pIFRK$^+$(3, 3) are more accurate than that of BE. Noting that IFRK(4, 4) has SSP coefficient $\mathcal{C} = 0$ and can not guarantee the strong stability for any $\tau > 0$, thus the time delay of pIFRK(4, 4) is obvious because the stabilization parameter is

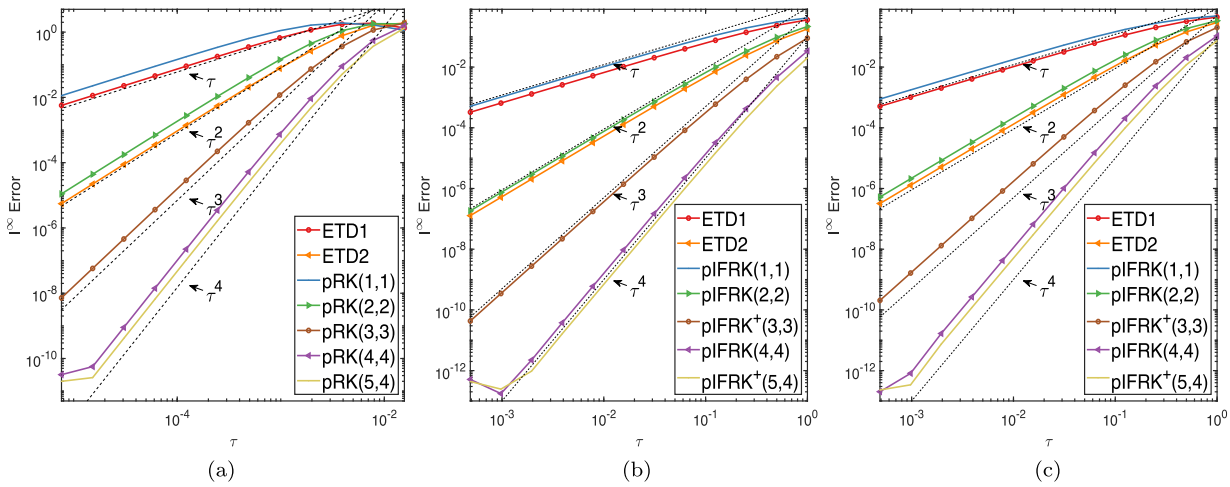

FIGURE 2. Time accuracy tests of pRK on the linear advection equation, and pIFRK on the Allen-Cahn equation. (a) pRK and ETD tests on (5.1), $\kappa = \frac{1}{\tau_{FE}} = 256$; (b) pIFRK and ETD tests on (5.3), $\kappa = 1$; (c) pIFRK and ETD tests on (5.3), $\kappa = 2$.

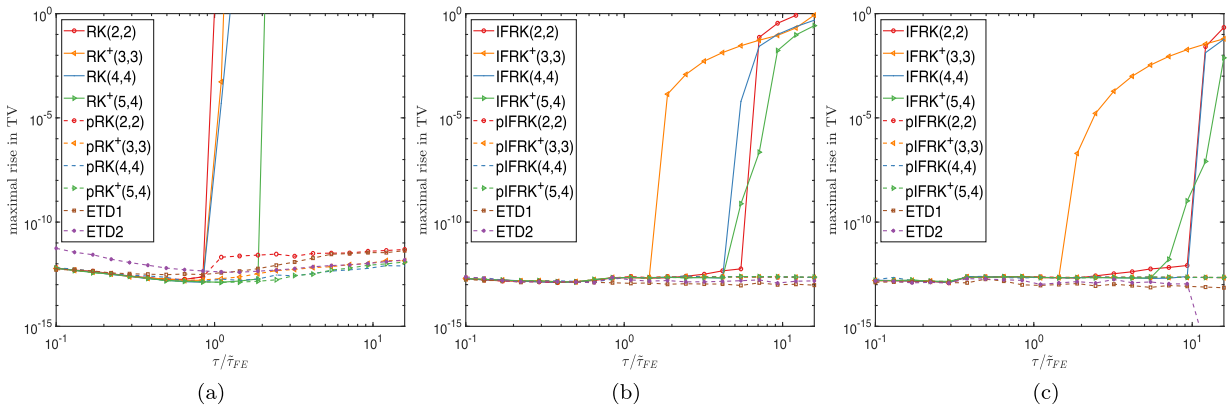

FIGURE 3. Example 5.3: The maximum rise in TV computed by different schemes. Parameters: $N = 1000$, $\kappa = 0, \max\left\{\frac{1}{\tilde{\tau}_{\mathrm{FE}}} - \frac{\mathcal{C}}{\tau}, 0\right\}, \frac{1}{\tilde{\tau}_{\mathrm{FE}}}$ for IFRK, pIFRK and ETD1/2 schemes, respectively. (a) $a = 0$, (b) $a = 5$ and (c) $a = 10$.

larger than those for pIFRK(2, 2) and pIFRK$^+$(3, 3). This is what we call stabilization trades consistency for stability.

In Figure 4(b), we choose a critical large time-step size $\tau = 0.0024 > \mathcal{C}\tilde{\tau}_{\mathrm{FE}}$ for all IFRK schemes. It demonstrates that the BE scheme introduces severe smoothing effect to the solution because of its low order, and the standard IFRK$^+$(5, 4) generates oscillations for this time step. Since the solutions of IFRK(2, 2), IFRK$^+$(3, 3) and IFRK(4, 4) blow up at this time step size, we do not present their solutions. On the contrary, the pIFRK(2, 2) scheme with a proper κ makes the solution stable, but large time delay appears because of introduced truncation errors. With the increasing of temporal convergence order, the solution delay of pIFRK becomes weaker, and the fourth-order pIFRK$^+$(5, 4) provides more accurate solution than the backward Euler scheme. This shows the superiority of the fourth-order pIFRK$^+$(5, 4) scheme over lower-order schemes, which is one main

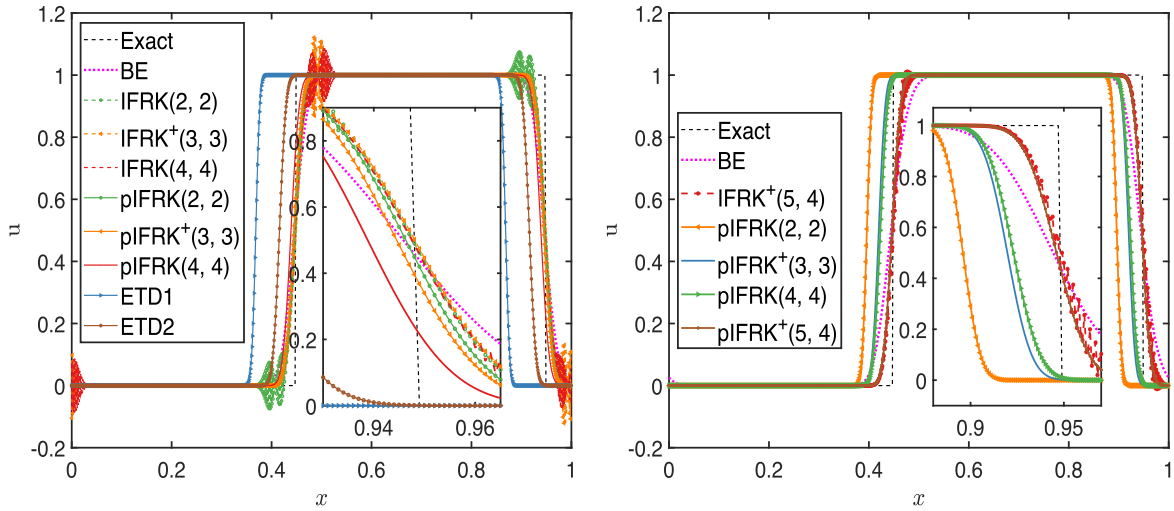

(a) (b)

FIGURE 4. Example 5.3: Solutions computed by BE, IFRK and pIFRK with different underlying RK Butcher tableaux. Parameters: $a = 0.1$; $N = 1000$; $\kappa = 0, \max\{\frac{1}{\tilde{\tau}_{FE}} - \frac{\mathcal{C}}{\tau}, 0\}, \frac{1}{\tilde{\tau}_{FE}}$ for IFRK, pIFRK and ETD1/2 schemes, respectively. (a) BE, ETD1/2: $\tau = 0.00113$; (p)IFRK$(2,2)$: $\tau = 0.00113$; (p)IFRK$^+(3,3)$: $\tau = 0.001355$; (p)IFRK$(4,4)$: $\tau = 0.00151$. (b) $\tau = 0.0024$ for all schemes.

TABLE 3. Ratios of τ and the allowable time steps $\mathcal{C}\tilde{\tau}_{\text{FE}}$ in Example 5.3. Parameters: $\tau = 0.0024$, $\tilde{\tau}_{\text{FE}} = 0.001$.

Underlying schemes	RK(2, 2)	RK$^+$(3, 3)	RK(4, 4)	RK$^+$(5, 4)	Backward Euler
$\mathcal{C}$ (IFRK)	1.0	$\frac{3}{4}$	0	1.3466	$\mathcal{C} = \infty$
Ratio ($\frac{\tau}{\mathcal{C}\tilde{\tau}_{\text{FE}}}$, pIFRK)	2.4	3.2	∞	1.78	
CPU time [s] (pIFRK)	0.025	0.045	0.070	0.091	CPU time = 0.46 [s]

contribution of this work. If we further increase the time step to a very large value, we point out that pIFRK$^+$(5, 4) will suffer from stronger time delay and may become less accurate than BE method, thus the time step of parametric schemes should be restricted by the prescribed accuracy. To further reduce the time delay at large time steps, the fourth-order pIFRK method with more stages [34] could be used. The ratios of this time step and the allowable time steps for the pIFRK schemes, as well as the CPU time costs are presented in Table 3. Because of the explicitness, the pIFRK schemes are more efficient than the backward Euler method. This is what we mean the pIFRK schemes are efficient inequality-preserving.

5.3. Maximum-principle-preserving tests

Example 5.4. Consider the evolution of the AC equation with the 1D profile given by the periodical boundary conditions and the smooth initial value (5.3). We set $\epsilon = 0.01$, and the final time $T = 100$.

In addition to the maximum principle, another intrinsic property of the AC equation is the dissipation of energy, *i.e.*,

$$\frac{\mathrm{d}}{\mathrm{d}t}E(u) = \left(\frac{\delta E(u)}{\delta u}, u_t\right) = -\left(\frac{\partial u}{\partial t}, \frac{\partial u}{\partial t}\right) \leq 0, \quad \forall t \in [0, T].$$

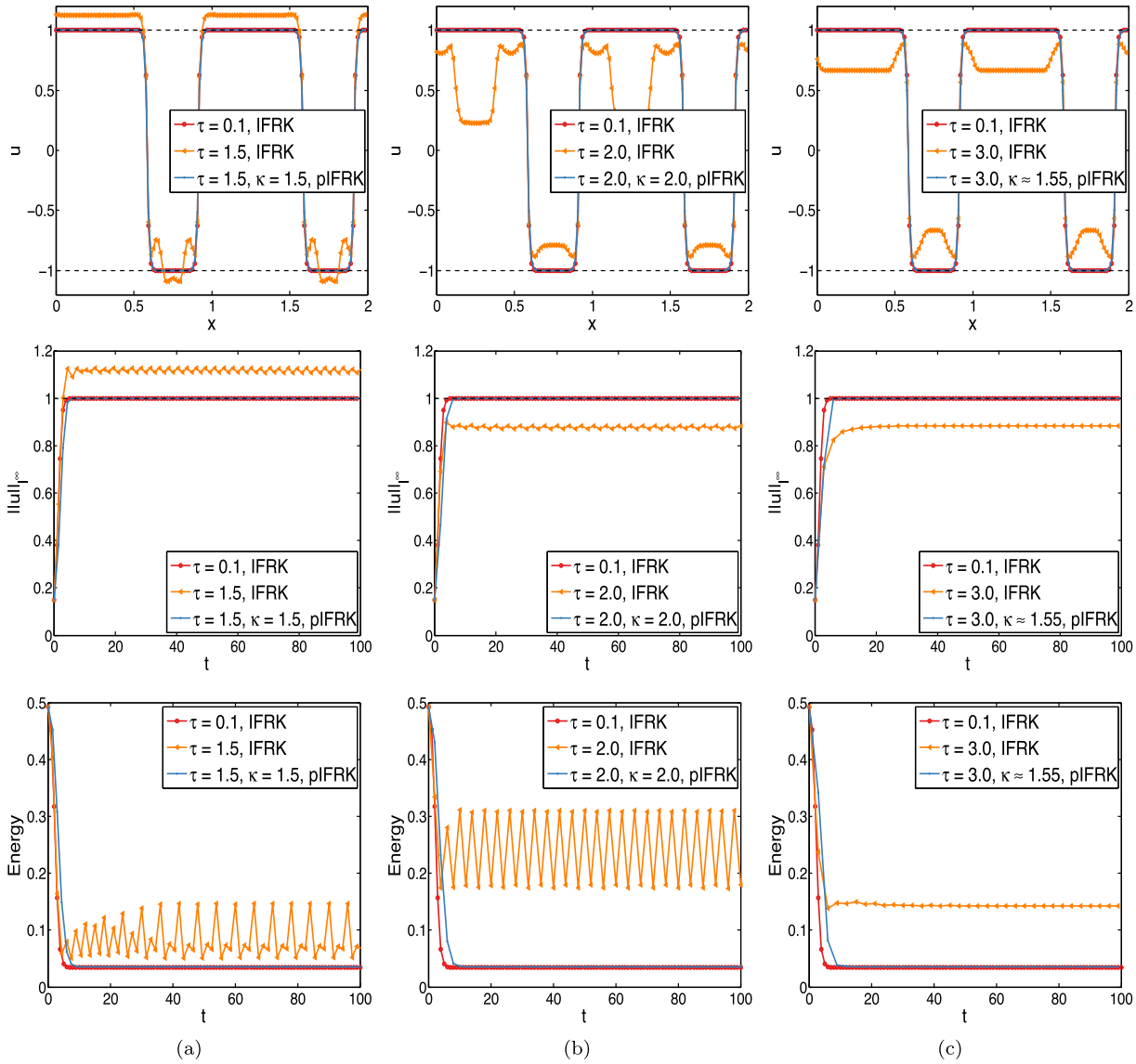

FIGURE 5. Example 5.4: The profiles of $\boldsymbol{u}$ (first row), evolutions of $\|\boldsymbol{u}\|_{l^\infty}$ (second row), and energy (third row) computed with different combinations of τ and κ using IFRK and pIFRK. Black dashed lines in the first and second rows denote the levels of ± 1. Parameters: $\epsilon = 0.01$, $N = 128$, $\kappa = 2 - \frac{C}{\tau}$ for the pIFRK schemes, and $\kappa = 0$ for IFRK schemes. (a) RK$^+$(3, 3), (b) RK$^+$(4, 4) and (c) RK$^+$(5, 4).

where $(\cdot,\cdot)$ denotes the L^2 inner product, *i.e.*, $(u,v) = \int_\Omega uv\mathrm{d}x$, and the energy functional is given by

$$E(u) = \int_\Omega \left(\frac{1}{2}\epsilon^2|\nabla u|^2 + \frac{(u^2-1)^2}{4}\right)\mathrm{d}x. \tag{5.4}$$

We test the third- and fourth-order integrators on the second-order central finite difference semi-discrete system. For a d-dimensional space, we denote the l^2-inner product by $\langle \boldsymbol{u}, \boldsymbol{v}\rangle := h^d \boldsymbol{v}^T\boldsymbol{u} = h^d \sum_{j=0}^{N-1} u_j v_j$,

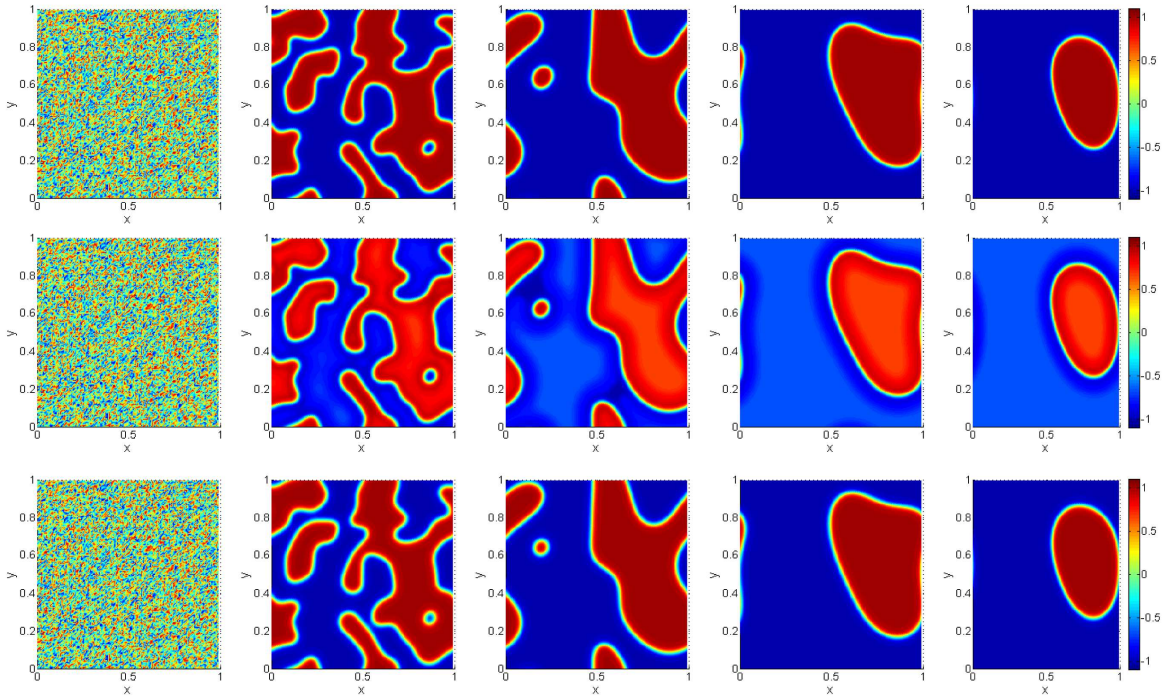

(a) (b) (c) (d) (e)

FIGURE 6. Example 5.5: Snapshots of solutions of AC equation. Top row: IFRK$^+$(5, 4), $\tau = 0.1$; middle row: IFRK$^+$(5, 4), $\tau = 3.0$; bottom row: pIFRK$^+$(5, 4), $\tau = 3.0, \kappa \approx 1.55$. Parameters: $\epsilon = 0.01$, $N = 128^2$. (a) RK$^+$(3, 3), (b) RK(4, 4) and (c)RK$^+$(5, 4).

then the energy functional (5.4) is discretized as $E_h(\boldsymbol{u}) = -\frac{1}{2}\langle L\boldsymbol{u}, \boldsymbol{u}\rangle + \langle \frac{(\boldsymbol{u}^2-1)^2}{4}, \mathbf{1}\rangle$. The solution profiles, evolutions of $\|\boldsymbol{u}\|_{l^\infty}$, and energy profiles are presented in Figure 5. Figure 5 column (a) presents the results of the AC equation computed with underlying RK$^+$(3, 3) scheme. We can observe that when the time step size τ increases from 0.1 to 1.5, IFRK$^+$(3, 3) produces oscillations in the solution (first row) and energy (third row) profiles, finally breaking the maximum principle (second row). By introducing a stabilization term with $\kappa = \frac{1}{\tilde{\tau}_{\mathrm{FE}}} - \frac{\mathcal{C}}{\tau} = 1.5$, the solution computed by pIFRK$^+$(3, 3) with $\tau = 1.5$ is not only accurate but also preserves the maximum-principle, and dissipates the energy. When adopting the fourth-order underlying RK(4, 4) scheme, although Figure 5 column (b) shows that the solution computed using IFRK(4, 4) with $\tau = 2.0$ does not break the maximum principle, the solution profile is no longer accurate (first row), and oscillations appear in the energy profile. With the introduction of $\kappa = 2.0$, pIFRK(4, 4) gives an accurate solution and well preserves such inequality structures. The results computed by the fourth-order schemes with underlying RK$^+$(5, 4) Butcher tableau are presented in column (c) of Figure 5. Similar as those in column (b), the solution of IFRK$^+$(5, 4) with $\tau = 3.0$ has oscillations. With suitable approximations of the exponential functions, we can see that the pIFRK$^+$(5, 4) scheme with $\tau = 3.0$ and $\kappa = \frac{1}{\tilde{\tau}_{\mathrm{FE}}} - \frac{\mathcal{C}}{\tau} \approx 1.55$ gives an accurate solution, preserves the maximum principle, and dissipates the energy. In addition, there is little difference between the computed solution and the reference solution obtained with $\tau = 0.1$.

Example 5.5. Consider the evolution of the 2D random profile given by

$$u(x, y, 0) = 1.90 \times \mathrm{rand}(x, y) - 0.95, \quad \Omega = (0, 1)^2,$$

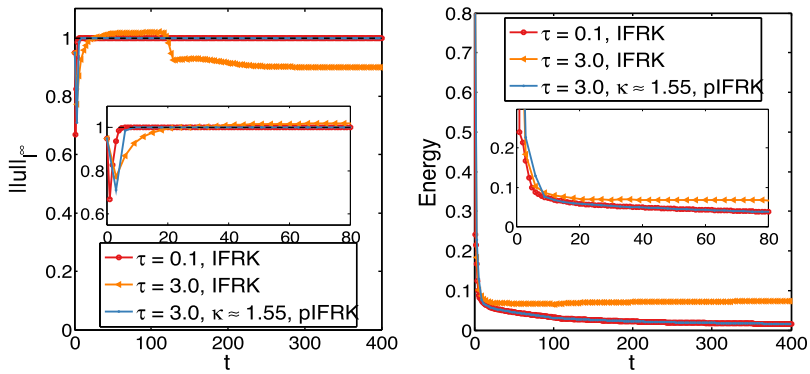

(a) (b)

FIGURE 7. Example 5.5: Evolutions of $\|\boldsymbol{u}\|_{l^\infty}$ (*left*), and energy E_h (*right*) of AC equation computed by IFRK$^+$(5, 4) and pIFRK$^+$(5, 4) with different τ and κ. Black dashed line in (a) denotes the maximum bound $\beta = 1$. Parameters: $N = 128^2$.

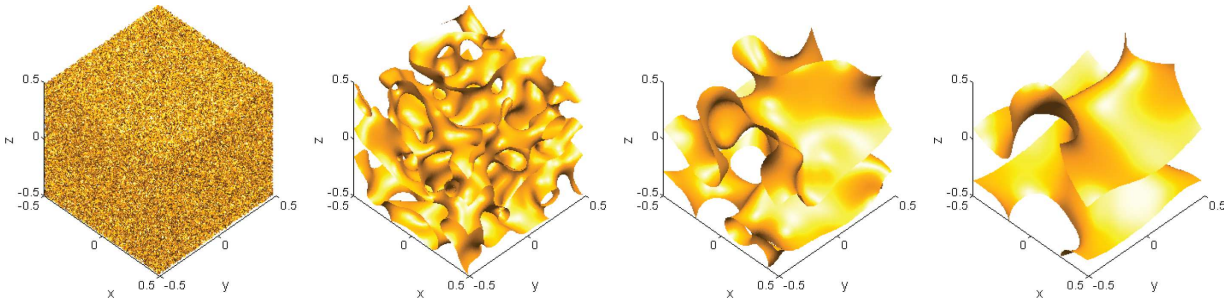

(a) (b) (c) (d)

FIGURE 8. Example 5.6: Isosurface snapshots of solutions at $t = 0,\ 30,\ 150$ and 360 computed by pIFRK$^+$(5, 4). Parameters: $N = 128^3$, $\tau = 3.0$ and $\kappa \approx 1.55$.

with periodic boundary conditions. Here and below, the rand() function is uniformly distributed in the interval $(0, 1)$.

By choosing $\epsilon = 0.01$, and discretizing the domain using $N = 128^2$ grid points. We solve the AC equation to final time $T = 400$ using the fourth-order schemes with underlying RK$^+$(5, 4) Butcher tableau. Figure 6 presents the initial profile and the zero-level set snapshots at $t = 0,\ 15,\ 90,\ 240,\ 390$ computed by IFRK$^+$(5, 4) and pIFRK$^+$(5, 4). The evolutions of $\|\boldsymbol{u}\|_{l^\infty}$ and discrete energy are presented in Figure 7. As τ increases from 0.1 to 3.0, oscillations appear in the solution profile (second row of Figs. 6 and 7(a)), and the energy profile deviates from the reference one computed with $\tau = 0.1$. Contrarily, by introducing the stabilization term with $\kappa \approx 1.55$, the pIFRK$^+$(5, 4) scheme with $\tau = 3.0$ preserves the maximum principle in Figure 7(a) and dissipates the energy in Figure 7(b). In Figure 6, the pIFRK$^+$(5, 4) solutions (bottom row) closely follow the reference ones in the top row. This clearly demonstrates the superiority of the proposed pIFRK schemes.

Example 5.6. At last, we consider the 3D AC equation with a uniformly random distributed phase field as the initial condition:

$$u(x, y, z, 0) = 1.8 \times \text{rand}(x, y, z) - 0.9, \quad \Omega = (-0.5, 0.5)^3.$$

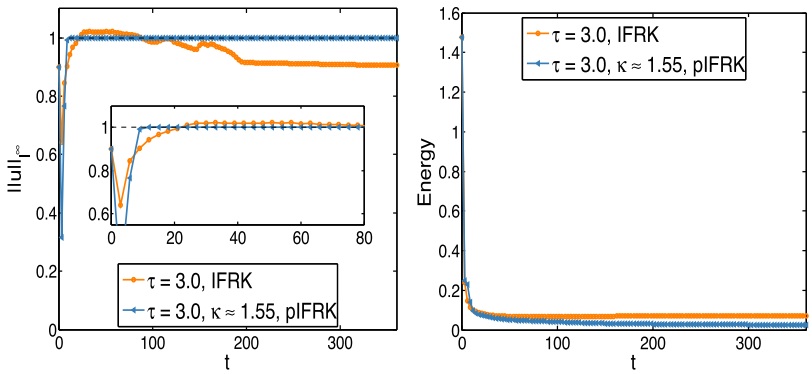

FIGURE 9. Example 5.6: Evolutions of $\|\boldsymbol{u}\|_{l^\infty}$ (*left*), and energy E_h (*right*) computed by using IFRK$^+$(5, 4) ($\tau = 3.0$) and pIFRK$^+$(5, 4) ($\tau = 3.0, \kappa \approx 1.55$); black dashed line denotes level of 1. Parameters: $N = 128^3$.

We set $\epsilon = 0.01$, and discretize the 3D domain using $N = 128^3$ grid points. The 3D isosurfaces computed by the fourth-order pIFRK$^+$(5, 4) scheme at $t = 0$, 30, 150 and 360 are presented in Figure 8. Figure 9 shows the evolutions of $\|\boldsymbol{u}\|_{l^\infty}$, and discrete energy E_h computed by IFRK$^+$(5, 4) and pIFRK$^+$(5, 4). It can be seen that the solution computed with $\tau = 3.0$ using IFRK$^+$(5, 4) violates the maximum-principle. In contrast, the pIFRK$^+$(5, 4) scheme with $\tau = 3.0, \kappa \approx 1.55$ well preserves the maximum-principle, and the energy profile is always decreasing.

6. Concluding remarks

In this paper we proposed a unified approach to develop up to the fourth-order inequality-preserving schemes for differential equations satisfying forward Euler conditions. One distinctive feature of the proposed schemes is the treatment of the stabilization term. By introducing a time-step-dependent stabilization parameter and taking advantage of the integrating factor method, we proposed approximating the exponential terms containing the stabilization parameter using novel recurrent approximations. Consequently, high-order fixed-point-preserving schemes were constructed. The presented order conditions showed that the pRK schemes retain the original convergence orders of underlying RK schemes used in this paper. Together with forward Euler conditions, we derived that the proposed schemes preserve the corresponding inequalities when $\kappa \geq \max\left\{\frac{1}{\tau_{\mathrm{FE}}} - \frac{\mathcal{C}}{\tau}, 0\right\}$. This restriction on κ is weaker than those required in existing ETD1/2 schemes, *i.e.*, $\kappa \geq \frac{1}{\tau_{\mathrm{FE}}}$, thus reducing additional truncation errors. To remove the requirement of a large stabilization parameter caused by the stiff linear term, we further developed pIFRK schemes by introducing the stiff operator in exponential functions. Linear stability analysis showed that proposed pRK schemes have good stability when suitable parameters are chosen. Numerical experiments on some typical advection equations and the Allen–Cahn equation were also carried out in this work, which demonstrated the robustness of proposed schemes, and verified the theoretical preservation of strong stability and maximum principle.

Because of the particularity of selected problems, the introduced stabilization term is of the form $\kappa(u - u)$, it is also meaningful to investigate the pRK approach for general nonlinear problems [58], *e.g.*, the mean curvature equation [57] or the Cahn–Hilliard equation [54], where different stabilization terms are introduced to allow large time-step sizes. Furthermore, as has been recognized in the references [8, 46, 48, 63, 85], the technique of adding and subtracting a stabilization term $-\kappa u$, $\kappa > 0$ to and from a system indeed trades consistency for stability by rescaling the time steps, and consequently time-delay appears as a by-product. Since it is a nontrivial task to remove the rescaling effects or estimate the correct rescaled time steps of pIFRK and ETD1/2, we will deal with such issues in a future work.

Appendix A. Proof of Lemma 2.1

Proof. We briefly illustrate the proof by taking the strong stability (2.6) as an example.

For a given $u^0 \in \mathbb{R}^N$ and $t_0 > 0$, denote $X_{u^0} = \{v \in \mathbb{R}^N | \|v\| \le \|u^0\|\}$ and $C([0,t_0]; X_{u^0}) = \{v : [0,t_0] \to X_{u^0} | v \text{ is continuous}\}$. Note that the forward Euler condition (1.2) on strong stability is equivalent to the circle condition,

$$\|\kappa u + f(t,u)\| \le \kappa \|u\| \le \kappa \|u^0\|, \qquad \forall \kappa \ge \frac{1}{\tau_{\mathrm{FE}}}, \forall t \in [0,T], \quad \forall \|u\| \le \|u^0\|.$$

Let $\kappa \ge \frac{1}{\tau_{\mathrm{FE}}}$, for a given $v \in C([0,t_0]; X_{u^0})$, we define $w : [0,t_0] \to \mathbb{R}^N$ as the solution to the system

$$\begin{cases} w_t = -\kappa w + f(t,v) + \kappa v, & t \in [0,t_0], \\ w(0) = u^0. \end{cases} \tag{A.1}$$

Then w is uniquely defined because of the linearity of (A.1). By Duhamel's formula, we have

$$w(t) = \mathrm{e}^{-\kappa t} u^0 + \int_0^t \mathrm{e}^{-\kappa(t-s)} \left[f(s, v(s)) + \kappa v(s) \right] \mathrm{d}s, \quad t \in [0,t_0]. \tag{A.2}$$

Taking $\|\cdot\|$ on both sides of (A.2) yields

$$\|w(t)\| \le \mathrm{e}^{-\kappa t}\|u^0\| + \int_0^t \mathrm{e}^{-\kappa(t-s)} \|f(s,v(s)) + \kappa v(s)\| \mathrm{d}s \le \mathrm{e}^{-\kappa t}\|u^0\| + \int_0^t \mathrm{e}^{-\kappa(t-s)} \kappa \|u^0\| \mathrm{d}s = \|u^0\|, \quad t \in [0,t_0].$$

Therefore, $w \in C([0,t_0]; X_{u^0})$. Next we define a mapping $\mathcal{A} : C([0,t_0]; X_{u^0}) \to C([0,t_0]; X_{u^0})$ as $\mathcal{A}(v) = w$ through (A.1). We show that $\mathcal{A}$ is a contraction for sufficiently small t_0. Assume $v_1, v_2 \in C([0,t_0]; X_{u^0})$, $w_1 = \mathcal{A}(v_1)$ and $w_2 = \mathcal{A}(v_2)$, then we obtain

$$w_1(t) - w_2(t) = \int_0^t \mathrm{e}^{-\kappa(t-s)} \left[f(s,v_1(s)) + \kappa v_1(s) - f(s,v_2(s)) - \kappa v_2(s) \right] \mathrm{d}s.$$

Since $f(t,u)$ satisfies the Lipschitz condition (2.1), we can derive

$$\begin{aligned} \|f(s,v_1(s)) + \kappa v_1(s) - f(s,v_2(s)) - \kappa v_2(s)\|_* &\le \|f(s,v_1(s)) - f(s,v_2(s))\|_* + \|\kappa v_1(s) - \kappa v_2(s)\|_* \\ &\le (K+\kappa) \|v_1(s) - v_2(s)\|_*. \end{aligned}$$

Then it holds that

$$\begin{aligned} \|w_1(t) - w_2(t)\|_* &\le \int_0^t \mathrm{e}^{-\kappa(t-s)} (K+\kappa) \|v_1(s) - v_2(s)\|_* \mathrm{d}s, \\ &\le \frac{K+\kappa}{\kappa} (1 - \mathrm{e}^{-\kappa t_0}) \|v_1 - v_2\|_{*, C\left([0,t_0]; X_{u^0}\right)}, \quad \forall t \in [0,t_0]. \end{aligned}$$

If $t_0 < \frac{1}{\kappa} \ln \frac{K+\kappa}{K}$, we have $\frac{K+\kappa}{\kappa}(1 - \mathrm{e}^{-\kappa t_0}) < 1$, and

$$\|\mathcal{A}(v_1) - \mathcal{A}(v_2)\|_{*, C\left([0,t_0]; X_{u^0}\right)} < \|v_1 - v_2\|_{*, C([0,t_0]; X_{u^0})},$$

then $\mathcal{A}$ is a contraction. Since X_{u^0} is closed in $\mathbb{R}^N$, thus $C([0,t_0]; X_{u^0})$ is complete with respect to the metric induced by the norm $\|\cdot\|_{*, C([0,t_0]; \mathbb{R}^N)}$, then Banach's fixed point theorem gives a unique fixed point $u \in C([0,t_0]; X_{u^0})$ of $\mathcal{A}(u) = u$, which is the unique solution to the equation (1.1). Continuing the process, we have the global existence of the unique solution $u \in C([0,T]; X_{u^0})$.

The properties in (2.7)–(2.10) can be proved similarly. □

Appendix B. Equivalence of the contraction semi-group property and the forward Euler condition

We show that the contraction semi-group condition on L in Assumption 1.1 is equivalent to the forward Euler condition (3.28) on Lu.

Lemma B.1 (Lemma 1a in [86]). *For any matrix $A = [a_{i,j}] \in \mathbb{R}^{N\times N}$, we define the logarithmic norm of A by*

$$\mu_\infty(A) = \lim_{\tau\to 0^+} \frac{\ln \|\mathrm{e}^{\tau A}\|_\infty}{\tau}. \tag{B.1}$$

Then the logarithmic norm can be calculated by $\mu_\infty(A) = \max_i \left\{a_{i,i} + \sum_{j\neq i} |a_{i,j}|\right\}$.

Lemma B.2. *The condition that $L \in \mathbb{R}^{N\times N}$ is the generator of a contraction semigroup on $\mathbb{R}^N$, that is, $\|\mathrm{e}^{\tau L}\|_\infty \le 1,\ \forall \tau > 0$, is equivalent to the forward Euler condition (3.28) on Lu.*

Proof. First, assume that the condition $\|\mathrm{e}^{\tau L}\|_\infty \le 1, \forall \tau > 0$ holds. By applying the sign-preservation of the limit in (B.1), we derive that $\mu_\infty(L) \le 0$. Applying Lemma B.1 yields

$$\mu_\infty(L) = \max_i \left\{ l_{i,i} + \sum_{j\neq i} |l_{i,j}| \right\} \le 0.$$

That is $l_{i,i} + \sum_{j\neq i} |l_{i,j}| \le 0$ and $l_{i,i} \le 0, i = 1, \ldots, N$.

If all $l_{i,i} = 0$, we can conclude that L is a zero matrix, and (3.28) holds for any $\bar{\tau}_{\mathrm{FE}} > 0$. Consider that there exists at least one $l_{i,i} < 0$. Let $\bar{\tau}_{\mathrm{FE}} = \min_i \left\{-\frac{1}{l_{i,i}}\right\}$ and $0 < \tau \le \bar{\tau}_{\mathrm{FE}}$, it can be derived that $1 + \tau l_{i,i} \ge 0, i = 1, \ldots, N$. Then we obtain

$$\begin{aligned}
\|I + \tau L\|_\infty &= \max_i \left\{ \left| 1 + \tau \left(l_{i,i} + \sum_{j\neq i} l_{i,j} \right) \right| \right\} \\
&\le \max_i \left\{ |1 + \tau l_{i,i}| + \tau \sum_{j\neq i} |l_{i,j}| \right\} \\
&= \max_i \left\{ 1 + \tau \left(l_{i,i} + \sum_{j\neq i} |l_{i,j}| \right) \right\} \\
&\le 1.
\end{aligned}$$

Then, we have

$$\|u + \tau L u\|_{l^\infty} \le \|I + \tau L\|_\infty \|u\|_{l^\infty} \le \|u\|_{l^\infty}, \quad \forall 0 < \tau \le \bar{\tau}_{\mathrm{FE}}.$$

Conversely, assume the forward Euler condition (3.28) on Lu holds. Let $r > 0$, we obtain

$$\left\|\mathrm{e}^{\tau L} u\right\|_{l^\infty} = \left\|\mathrm{e}^{-r}\mathrm{e}^{rI+\tau L} u\right\|_{l^\infty} \le \mathrm{e}^{-r} \sum_{k=0}^{\infty} \frac{r^k}{k!} \left\| \left(I + \frac{\tau}{r} L\right)^k u \right\|_{l^\infty} \le \mathrm{e}^{-r} \sum_{k=0}^{\infty} \frac{r^k}{k!} \|u\|_{l^\infty} = \|u\|_{l^\infty}, \quad \forall \tau \le r\bar{\tau}_{\mathrm{FE}}.$$

Since r can be arbitrarily large, then we have $\|\mathrm{e}^{\tau L}\|_\infty \le 1, \ \forall \tau > 0$.

This completes the proof. □

Acknowledgements. This work was supported by the National Natural Science Foundation of China (Nos. 12271523, 11901577, 11971481, 12071481), the Defense Science Foundation of China (2021-JCJQ-JJ-0538), Science and Technology Innovation Program of Hunan Province (2022RC1192, 2021RC3082), National Key R&D Program of China (SQ2020YFA0709803), and fund of National University of Defense Technology (ZK19-37).

References

[1] S. Gottlieb, D.I. Ketcheson and C.-W. Shu, Strong stability preserving Runge–Kutta and multistep time discretizations, World Scientific (2011).

[2] J.F.B.M. Kraaijevanger, Contractivity of Runge–Kutta methods. *BIT Numer. Math.* **31** (1991) 482–528.

[3] L. Bonaventura and A. Della Rocca, Unconditionally strong stability preserving extensions of the TR-BDF2 method. *J. Sci. Comput.* **70** (2017) 859–895.

[4] Q. Du, L. Ju, X. Li and Z. Qiao, Maximum bound principles for a class of semilinear parabolic equations and exponential time-differencing schemes. *SIAM Rev.* **63** (2021) 317–359.

[5] C.-W. Shu, Total-variation-diminishing time discretizations. *SIAM J. Sci. Stat. Comput.* **9** (1988) 1073–1084.

[6] X. Zhang and C.-W. Shu, Positivity-preserving high order finite difference WENO schemes for compressible Euler equations. *J. Comput. Phys.* **231** (2012) 2245–2258.

[7] X. Zhang and C.-W. Shu, On maximum-principle-satisfying high order schemes for scalar conservation laws. *J. Comput. Phys.* **229** (2010) 3091–3120.

[8] J. Huang and C.-W. Shu, Bound-preserving modified exponential Runge–Kutta discontinuous Galerkin methods for scalar hyperbolic equations with stiff source terms. *J. Comput. Phys.* **361** (2018) 111–135.

[9] W. Hundsdorfer, S.J. Ruuth and R.J. Spiteri, Monotonicity-preserving linear multistep methods. *SIAM J. Numer. Anal.* **41** (2003) 605–623.

[10] L. Ferracina and M.N. Spijker, Stepsize restrictions for the total-variation-diminishing property in general Runge–Kutta methods. *SIAM J. Numer. Anal.* **42** (2004) 1073–1093.

[11] L. Ferracina and M. Spijker, An extension and analysis of the Shu–Osher representation of Runge–Kutta methods. *Math. Comput.* **74** (2005) 201–219.

[12] I. Higueras, On strong stability preserving time discretization methods. *J. Sci. Comput.* **21** (2004) 193–223.

[13] I. Higueras, Representations of Runge–Kutta methods and strong stability preserving methods. *SIAM J. Numer. Anal.* **43** (2005) 924–948.

[14] S.J. Ruuth and R.J. Spiteri, Two barriers on strong-stability-preserving time discretization methods. *J. Sci. Comput.* **17** (2002) 211–220.

[15] H.W. Lenferink, Contractivity preserving explicit linear multistep methods. *Numer. Math.* **55** (1989) 213–223.

[16] J. Sand, Circle contractive linear multistep methods. *BIT Numer. Math.* **26** (1986) 114–122.

[17] R.J. Spiteri and S.J. Ruuth, A new class of optimal high-order strong-stability-preserving time discretization methods. *SIAM J. Numer. Anal.* **40** (2002) 469–491.

[18] D.I. Ketcheson, C.B. Macdonald and S. Gottlieb, Optimal implicit strong stability preserving Runge–Kutta methods. *Appl. Numer. Math.* **59** (2009) 373–392.

[19] G. Izzo and Z. Jackiewicz, Strong stability preserving general linear methods. *J. Sci. Comput.* **65** (2015) 271–298.

[20] M. Spijker, Contractivity in the numerical solution of initial value problems. *Numer. Math.* **42** (1983) 271–290.

[21] A. Bellen and L. Torelli, Unconditional contractivity in the maximum norm of diagonally split Runge–Kutta methods. *SIAM J. Numer. Anal.* **34** (1997) 528–543.

[22] K.J. in't Hout, A note on unconditional maximum norm contractivity of diagonally split Runge–Kutta methods. *SIAM J. Numer. Anal.* **33** (1996) 1125–1134.

[23] C.B. Macdonald, S. Gottlieb and S.J. Ruuth, A numerical study of diagonally split Runge–Kutta methods for PDEs with discontinuities. *J. Sci. Comput.* **36** (2008) 89–112.

[24] D.I. Ketcheson, Step sizes for strong stability preservation with downwind-biased operators. *SIAM J. Numer. Anal.* **49** (2011) 1649–1660.

[25] S. Gottlieb, Z.J. Grant, J. Hu and R. Shu, High order unconditionally strong stability preserving multi-derivative implicit and IMEX Runge–Kutta methods with asymptotic preserving properties. Preprint arXiv:2102.11939 (2021).

[26] S. Blanes, A. Iserles and S. Macnamara, Positivity-preserving methods for ordinary differential equations. *ESAIM: Math. Model. Numer. Anal.* **56** (2022) 1843–1870.

[27] S. Ortleb and W. Hundsdorfer, Patankar-type Runge–Kutta schemes for linear PDEs, in *AIP Conference Proceedings*, Vol. 1863, AIP Publishing LLC (2017) 320008.

[28] S. Kopecz and A. Meister, Unconditionally positive and conservative third order modified Patankar–Runge–Kutta discretizations of production–destruction systems. *BIT Numer. Math.* **58** (2018) 691–728.

[29] J. Huang, T. Izgin, S. Kopecz, A. Meister and C.-W. Shu, On the stability of strong-stability-preserving modified Patankar Runge–Kutta schemes. Preprint arXiv:2205.01488 (2022).

[30] L. Ju, X. Li, Z. Qiao and J. Yang, Maximum bound principle preserving integrating factor Runge–Kutta methods for semilinear parabolic equations. *J. Comput. Phys.* **439** (2021) 110405.

[31] T. Tang and J. Yang, Implicit–explicit scheme for the Allen–Cahn equation preserves the maximum principle. *J. Comput. Math.* **34** (2016) 471–481.

[32] J. Shen, T. Tang and J. Yang, On the maximum principle preserving schemes for the generalized Allen–Cahn equation. *Commun. Math. Sci.* **14** (2016) 1517–1534.

[33] J. Shen and X. Zhang, Discrete maximum principle of a high order finite difference scheme for a generalized Allen–Cahn equation. *Commun. Math. Sci.* **20** (2022) 1409–1436.

[34] L. Isherwood, Z.J. Grant and S. Gottlieb, Strong stability preserving integrating factor Runge–Kutta methods. *SIAM J. Numer. Anal.* **56** (2018) 3276–3307.

[35] L. Isherwood, Z.J. Grant and S. Gottlieb, Downwinding for preserving strong stability in explicit integrating factor Runge–Kutta methods. *Pure Appl. Math. Q.* **14** (2018) 3–25.

[36] L. Isherwood, Z.J. Grant and S. Gottlieb, Strong stability preserving integrating factor two-step Runge–Kutta methods. *J. Sci. Comput.* **81** (2019) 1446–1471.

[37] H. Zhang, J. Yan, X. Qian and S. Song, Numerical analysis and applications of explicit high order maximum principle preserving integrating factor Runge–Kutta schemes for Allen–Cahn equation. *Appl. Numer. Math.* **161** (2021) 372–390.

[38] Q. Du, L. Ju, X. Li and Z. Qiao, Maximum principle preserving exponential time differencing schemes for the nonlocal Allen–Cahn equation. *SIAM J. Numer. Anal.* **57** (2019) 875–898.

[39] L. Ju, X. Li and Z. Qiao, Generalized SAV-exponential integrator schemes for Allen–Cahn type gradient flows. *SIAM J. Numer. Anal.* **60** (2022) 1905–1931.

[40] J. Li, X. Li, L. Ju and X. Feng, Stabilized integrating factor Runge–Kutta method and unconditional preservation of maximum bound principle. *SIAM J. Sci. Comput.* **43** (2021) A1780–A1802.

[41] H. Zhang, J. Yan, X. Qian, X. Chen and S. Song, Explicit third-order unconditionally structure-preserving schemes for conservative Allen–Cahn equations. *J. Sci. Comput.* **90** (2022) 1–29.

[42] H. Zhang, J. Yan, X. Qian and S. Song, Temporal high-order, unconditionally maximum-principle-preserving integrating factor multi-step methods for Allen–Cahn-type parabolic equations. *Appl. Numer. Math.* **186** (2023) 18–40.

[43] H. Zhang, J. Yan, X. Qian and S. Song, Up to fourth-order unconditionally structure-preserving parametric single-step methods for semilinear parabolic equations. *Comput. Methods Appl. Mech. Eng.* **393** (2022) 114817.

[44] H. Zhang, X. Qian, J. Xia and S. Song, Unconditionally maximum-principle-preserving parametric integrating factor two-step Runge–Kutta Schemes for parabolic sine-gordon equations. *CSIAM Trans. Appl. Math.* **4**(2023) 177–22.

[45] J. Du, C. Wang, C. Qian and Y. Yang, High-order bound-preserving discontinuous Galerkin methods for stiff multispecies detonation. *SIAM J. Sci. Comput.* **41** (2019) B250–B273.

[46] J. Du and Y. Yang, Third-order conservative sign-preserving and steady-state-preserving time integrations and applications in stiff multispecies and multireaction detonations. *J. Comput. Phys.* **395** (2019) 489–510.

[47] J. Du, E. Chung and Y. Yang, Maximum-principle-preserving local discontinuous Galerkin methods for Allen–Cahn equations. *Commun. Appl. Math. Comput.* **4** (2022) 353–379.

[48] R. Yang, Y. Yang and Y. Xing, High order sign-preserving and well-balanced exponential Runge–Kutta discontinuous Galerkin methods for the shallow water equations with friction. *J. Comput. Phys.* **444** (2021) 110543.

[49] J. Shen and X. Yang, Numerical approximations of Allen–Cahn and Cahn–Hilliard equations. *Discrete Contin. Dyn. Syst.* **28** (2010) 1669–1691.

[50] J. Douglas Jr. and T. Dupont, Alternating-direction Galerkin methods on rectangles, in Numerical Solution of Partial Differential Equations–II, Elsevier (1971) 133–214.

[51] D.J. Eyre, An unconditionally stable one-step scheme for gradient systems. Unpublished article (1998).

[52] P. Smereka, Semi-implicit level set methods for curvature and surface diffusion motion. *J. Sci. Comput.* **19** (2003) 439–456.

[53] C. Xu and T. Tang, Stability analysis of large time-stepping methods for epitaxial growth models. *SIAM J. Numer. Anal.* **44** (2006) 1759–1779.

[54] Y. He, Y. Liu and T. Tang, On large time-stepping methods for the Cahn–Hilliard equation. *Appl. Numer. Math.* **57** (2007) 616–628.

[55] C.B. Macdonald and S.J. Ruuth, The implicit closest point method for the numerical solution of partial differential equations on surfaces. *SIAM J. Sci. Comput.* **31** (2010) 4330–4350.

[56] C.-B. Schönlieb and A. Bertozzi, Unconditionally stable schemes for higher order inpainting. *Commun. Math. Sci.* **9** (2011) 413–457.

[57] K. Chow and S.J. Ruuth, Linearly stabilized schemes for the time integration of stiff nonlinear PDEs. *J. Sci. Comput.* **87** (2021) 1–29.

[58] M. Hochbruck, A. Ostermann and J. Schweitzer, Exponential Rosenbrock-type methods. *SIAM J. Numer. Anal.* **47** (2009) 786–803.

[59] W. Hundsdorfer, A note on stability of the Douglas splitting method. *Math. Comput.* **67** (1998) 183–190.

[60] L. Duchemin and J. Eggers, The explicit–implicit-null method: Removing the numerical instability of PDEs. *J. Comput. Phys.* **263** (2014) 37–52.

[61] H. Wang, Q. Zhang, S. Wang and C.-W. Shu, Local discontinuous Galerkin methods with explicit–implicit-null time discretizations for solving nonlinear diffusion problems. *Sci. China Math.* **63** (2020) 183–204.

[62] L. Ju, J. Zhang, L. Zhu and Q. Du, Fast explicit integration factor methods for semilinear parabolic equations. *J. Sci. Comput.* **62** (2015) 431–455.

[63] J. Xu, Y. Li, S. Wu and A. Bousquet, On the stability and accuracy of partially and fully implicit schemes for phase field modeling. *Comput. Methods Appl. Mech. Eng.* **345** (2019) 826–853.

[64] S. Krogstad, Generalized integrating factor methods for stiff PDEs. *J. Comput. Phys.* **203** (2005) 72–88.

[65] A. Ostermann, M. Thalhammer and W. Wright, A class of explicit exponential general linear methods. *BIT Numer. Math.* **46** (2006) 409–431.

[66] M. Bassenne, L. Fu and A. Mani, Time-accurate and highly-stable explicit operators for stiff differential equations. *J. Comput. Phys.* **424** (2021) 109847.

[67] M. Calvo, J.I. Montijano and L. Rández, A note on the stability of time–accurate and highly–stable explicit operators for stiff differential equations. *J. Comput. Phys.* **436** (2021) 110316.

[68] C.-W. Shu and S. Osher, Efficient implementation of essentially non-oscillatory shock-capturing schemes. *J. Comput. Phys.* **77** (1988) 439–471.

[69] S. Conde, S. Gottlieb, Z.J. Grant and J.N. Shadid, Implicit and implicit–explicit strong stability preserving Runge–Kutta methods with high linear order. *J. Sci. Comput.* **73** (2017) 667–690.

[70] J.C. Butcher, Trees and numerical methods for ordinary differential equations. *Numer. Algorithms* **53** (2010) 153–170.

[71] J.D. Lawson, Generalized Runge–Kutta processes for stable systems with large Lipschitz constants. *SIAM J. Numer. Anal.* **4** (1967) 372–380.

[72] Z. Jackiewicz, General Linear Methods for Ordinary Differential Equations, John Wiley & Sons (2009).

[73] H. Zhang, Repository to verify the order conditions of pRK. https://github.com/auseraccount/pRK (accessed 17 June 2022).

[74] S.M. Cox and P.C. Matthews, Exponential time differencing for stiff systems. *J. Comput. Phys.* **176** (2002) 430–455.

[75] S. Gottlieb and C.-W. Shu, Total variation diminishing Runge–Kutta schemes. *Math. Comput.* **67** (1998) 73–85.

[76] D. Li, Z. Qiao and T. Tang, Characterizing the stabilization size for semi-implicit Fourier-spectral method to phase field equations. *SIAM J. Numer. Anal.* **54** (2016) 1653–1681.

[77] A. Ostermann and M. Van Daele, Positivity of exponential Runge–Kutta methods. *BIT Numer. Math.* **47** (2007) 419–426.

[78] A. Ostermann and M. Thalhammer, Positivity of exponential multistep methods, in Numerical Mathematics and Advanced Applications, Springer (2006) 564–571.

[79] M. Hochbruck and A. Ostermann, Explicit exponential Runge–Kutta methods for semilinear parabolic problems. *SIAM J. Numer. Anal.* **43** (2005) 1069–1090.

[80] W. Hundsdorfer and J.G. Verwer, Numerical Solution of Time-Dependent Advection–Diffusion–Reaction Equations, Vol. 33, Springer Science & Business Media (2013).

[81] S. González-Pinto and D. Hernández-Abreu, Strong A-acceptability for rational functions. *BIT Numer. Math.* **43** (2003) 555–561.

[82] E. Hairer and G. Wanner, Solving Ordinary Differential Equations II. Springer Berlin, Heidelberg (1996).

[83] H. Wang, C.-W. Shu and Q. Zhang, Stability and error estimates of local discontinuous Galerkin methods with implicit-explicit time-marching for advection-diffusion problems. *SIAM J. Numer. Anal.* **53** (2015) 206–227.

[84] Q. Du, L. Ju and J. Lu, Analysis of fully discrete approximations for dissipative systems and application to time-dependent nonlocal diffusion problems. *J. Sci. Comput.* **78** (2019) 1438–1466.

[85] Y. Li, H.G. Lee, D. Jeong and J. Kim, An unconditionally stable hybrid numerical method for solving the Allen–Cahn equation. *Comput. Math. Appl.* **60** (2010) 1591–1606.

[86] T. Ström, On logarithmic norms. *SIAM J. Numer. Anal.* **12** (1975) 741–753.